Electronic Supplementary Information

Porphyrin Nanotubes based on Hydrogen-bonded Organic Framework

Sumra Idrees[a], Zhikai Li[b], Fang Fang[c], Huowang He[a], Irfan Majeed[a], Yihuan Zhang[a], Atsuhiro Osuka[d], Yan Cao*[e], Zhuo Zeng*[a], Xiaopeng Li*[b] and Hua-Wei Jiang*[a]

a. GDMPA Key Laboratory for Process Control and Quality Evaluation of Chiral Pharmaceuticals, School of Chemistry, South China Normal University, Guangzhou 510006, China
E-mail: zhuoz@scnu.edu.cn; hwjiang@m.scnu.edu.cn
b. College of Chemistry and Environmental Engineering, Shenzhen University, Shenzhen 518060, China
E-mail: xiaopengli@szu.edu.cn
c. Instrumental Analysis Center of Shenzhen University, Shenzhen University, Shenzhen 518060, China
d. Key Laboratory of the Assembly and Application of Organic Functional Molecules of Hunan Province, College of Chemistry and Chemical Engineering, Hunan Normal University, Changsha 410081, China
e. Institute for Advanced Study (IAS), Shenzhen University, Shenzhen 518060, China
E-mail: caoyan@szu.edu.cn

Table of Contents

1. Instrumentation and Materials

All the reagents and solvents were obtained from commercial suppliers and used as received without any further purification or distillation unless or otherwise it is noted. The nuclear magnetic resonance (NMR) spectra were recorded on a 600 MHz Bruker nuclear magnetic resonance spectrometer and solvent was chloroform ($CDCl_3$) unless otherwise specified. The chemical shifts (δ) were referenced with residual solvent signals at 7.26 ($CDCl_3$) for ^1H and at 77.16 ppm ($CDCl_3$) for ^{13}C-NMR. UV/Vis spectra were collected with a Shimadzu UV-2700 instrument. Optical spectra of precursors were recorded in dichloromethane, while of porphyrin nanotubes (PNTs) were recorded in ethanol, dimethyl sulfoxide (DMSO), 1,4-dioxane and toluene. SEM images were taken on a Field emission scanning electron microscope ZEISS Gemini 500 (FE-SEM). The samples were dispersed in toluene and costed a drop on silicon wafer adhered on the flat sample holder and then coated with platinum using sputter coater in inert atmosphere. The transmission electron microscopy was performed on 120 kV JEM-1400 PLUS, while HRTEM on 200 kV JOEL JEM-2100HR. The crystalline properties of PNTs were examined by selected-area electron diffraction (SAED) (Oxford Instruments IET250 spectrometer) and images were recorded by American Gatan company 832 CCD camera. The suspension of the PNTs sample was prepared in toluene, the solution was dropped on an ultra-thin carbon support film, and prior to observation the sample was heated at 50 ^oC under heating lamp to remove the solvent. The diameter of the nanotubes was measured by using Image J software and statistical analysis was applied by measuring the diameter not less than 30 different regions to give corresponding diameter distribution. Matrix-assisted laser desorption/ionization time-of-flight (MALDI-TOF) mass characterization was conducted on a Bruker UltrafleXtreme TOF/TOF mass spectrometer (Bruker Daltonics, Inc., Billerica, MA) equipped with a Nd: YAG laser (355 nm). Trans-2-[3-(4-tert-butylphenyl)-2-methyl-2-propenylidene] malononitrile (DCTB, Aldrich, >99%) was applied as matrix. The FTIR spectra were acquired on German Platinum Elmer Spectrum Two Fourier Transform Infrared Spectrometer. The samples were prepared as KBr pellets. The small and wide-angle X-ray diffraction (SAXD and WAXD) were performed on BRUKER D8 ADVANCE X-ray diffraction instrument. The thermogravimetric analysis (TGA) was recorded on NETZSCH TG 209 F3 Thermogravimetric Analyzer, and the self-assembled PNTs sample was heated at a rate of 10 °C/min up to 800 °C under N_2 atmosphere.The N_2 sorption isotherm measurements were carried out using a Micromeritics 3Flex Version 4.02 instrument.

2. Experimental Section

Synthesis of Precursors

From the precursors, 4-ethoxy carbonyl benzaldehyde[1] and dipyrromethane[2] the 5,15-bis(ethoxycarbonylphenyl)-porphyrin was synthesized according to the procedure already reported. Then Zn metallization and the bromination at *meso* positions of porphyrin was achieved according to literature method.[3] The crude product (**1-Br**) was further purified by recrystallization with CH_2Cl_2 / MeOH. The dibromo porphyrin (**1-Br**) was obtained as a dark purple solid (yield = 1.19 g, 90%).

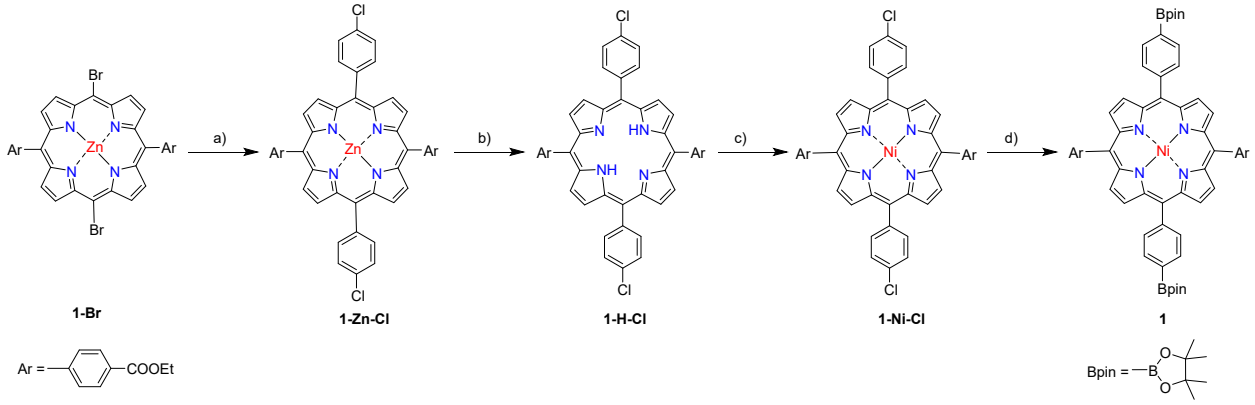

Scheme S1. Synthesis of **1**. Conditions: **a)** 2-(4-chlorophenyl)-4,4,5,5-tetramethyl-1,3,2-dioxaborolane, Pd $(PPh_3)_2Cl_2$, K_3PO_4, DMF, 90 °C, overnight; **b)** DCM, 1 mL HCl, rt 15 min.; **c)** $Ni(acac)_2$, toluene, reflux, 24 h; **d)** B_2pin_2, X-phos, KOAc, dioxane, reflux overnight.

5,15-bis(ethoxycarbonylphenyl)-10, 20-bis(parachlorophenyl)-Zn-porphyrin (1-Zn-Cl)

To a 100 mL two neck flask, corresponding porphyrin **1-Br** (500 mg, 0.604 mmol), 2-(4-chlorophenyl)4,4,5,5-tetramethyl-1,3,2-dioxaloborolane (720.4 mg, 3.02 mmol), Pd $(PPh_3)_2Cl_2$ (127.04 mg, 0.18 mmol and K_3PO_4 (1025.3 mg, 4.83 mmol） were added. The flask was degassed and purged with N_2 three times then anhydrous DMF (30 mL) was added. After refluxing at 90 °C for overnight, the reaction mixture was cooled down to room temperature and poured into cold water. The resulting solid precipitates were filtered and re-dissolved in DCM, followed by washing with water and saturated brine for three times (Scheme S1-a). The organic layer was dried with anhydrous Na_2SO_4 then mixture was evaporated to dryness and recrystalised with DCM/MeOH (dark purple solid, yield = 446 mg, 83%). **(1-Zn-Cl)** ^{1}H NMR (600 MHz, $CDCl_3$): δ (ppm) 8.95 (d, J = 4.7 Hz, 4H), 8.92 (d, J = 4.7 Hz, 4H), 8.45 (d, J = 8.0 Hz, 4H), 8.29 (d, J = 8.0 Hz, 4H), 8.14 (d, J = 8.3 Hz, 4H), 7.75 (d, J = 8.3 Hz, 4H), 4.58 (q, J = 7.2 Hz, 4H), 1.55 (t, J = 7.2 Hz, 6H); ^{13}C NMR (151 MHz, $CDCl_3$): δ (ppm) 167.00, 150.31, 149.97, 147.45, 141.15, 135.51, 134.52, 134.31, 132.32, 132.18, 131.58, 130.01, 129.19, 128.40, 127.95, 127.58, 127.06, 120.44, 120.22, 61.46, 14.64. UV-vis (CH_2Cl_2): λ/nm (ε/$M^{-1}cm^{-1}$) 421 (311000), and 549 (10000); MALDI-TOF MS *m/z* ($[M - e^-]^{+\cdot}$) 888.12, calculated for $C_{50}H_{34}Cl_2N_4O_4Zn$: 888.12.

De-metallization (1-H-Cl)

First for de-metallization of Zn (II), the above synthesised porphyrin **(1-Zn-Cl)** 500 mg (0.56 mmol) was dissolved in 130 mL of DCM. While stirring at room temperature, 1 mL of conc. HCl was added and allowed to stir further for 10 mins (Scheme S1-b). The reaction mixture was neutralized by saturated solution of $NaHCO_3$ and washed with water. Organic layer was separated and dried over anhydrous $NaSO_4$. After the evaporation of solvent, the product was passed through silica gel column to remove Zn (II) salt using DCM with 1% TEA as eluent (dark purple solid, yield = 410 mg, 88%). **(1-H-Cl)** ^{1}H NMR (600 MHz, $CDCl_3$): δ (ppm) 8.83 (m, 8H), 8.46 (d, *J* = 8.2 Hz, 4H), 8.30 (d, *J* = 8.2 Hz, 4H), 8.14 (d, *J* = 8.2 Hz, 4H), 7.75 (d, *J* = 8.2 Hz, 4H), 4.59 (q, *J* = 7.1 Hz, 4H), 1.55 (t, *J* = 7.1 Hz, 6H), -2.83 (s, 2H); ^{13}C NMR (151 MHz, $CDCl_3$): δ (ppm) 166.10, 146.73, 139.96, 135.63, 134.65, 134.58, 130.26, 128.10, 127.21, 119.48, 119.10, 61.52, 14.65; UV-vis (CH_2Cl_2): λ/nm (ε/$M^{-1}cm^{-1}$) 419 (327000), 516 (3800), 549 (3400), 590 (3100), and 646 (2700).

Ni-metallization (1-Ni-Cl)

A solution of free base porphyrin **1-H-Cl** 500 mg (0.604 mmol) and bis-(2,4-pentanediono) nickel salt 347 mg (1.347 mmol) in toluene (130 mL) was heated under reflux for 24 h (Scheme S1-c). After reaction completion, the solvent was evaporated under vacuum. The residue was dissolved in $CHCl_3$ and passed through a short silica gel column with $CHCl_3$ as eluent. The crude product was further purified by recrystallization from $CHCl_3$/MeOH (brick red solid, yield = 428 mg, 80%). **(1-Ni-Cl)** ^{1}H NMR (600 MHz, $CDCl_3$): δ (ppm) 8.74 (d, *J* = 4.9 Hz, 4H), 8.71 (d, *J* = 4.9 Hz, 4H), 8.38 (d, *J* = 8.1 Hz, 4H), 8.09 (d, *J* = 8.1 Hz, 4H), 7.93 (d, *J* = 8.3 Hz, 4H), 7.67 (d, *J* = 8.3 Hz, 4H), 4.55 (q, *J* = 7.2 Hz, 4H), 1.52 (t, *J* = 7.2 Hz, 6H); ^{13}C NMR (151 MHz, $CDCl_3$): δ (ppm) 166.83, 145.49, 142.83, 142.50, 139.25, 134.85, 134.54, 133.83, 132.48, 132.36, 130.30, 128.28, 127.39, 118.38, 118.15, 62.28, 14.62; UV-vis (CH_2Cl_2): λ/nm (ε/$M^{-1}cm^{-1}$) 416 (177000), and 529 (16000); MALDI-TOF MS *m/z* ($[M - e^-]^{+\cdot}$) 882.13, calculated for $C_{50}H_{34}Cl_2N_4NiO_4$: 882.13.

Precursor 1

Borylation of **1-Ni-Cl** porphyrin was achieved through literature method reported by S.L Buchwald et al.[4] To a 25 mL two neck flask all dry reagents including, Ni porphyrin (150 mg, 0.169 mmol), B_2pin_2 (430.6 mg, 1.696 mmol), Pd $(OAc)_2$ (7.6 mg, 0.034 mmol), KOAc (199.2 mg, 2.03 mmol) and X-Phos (32.23 mg, 0.0676 mmol) were added. The flask was degassed and purged with argon three times. The anhydrous 1,4-dioxane (5 mL) was added and the reaction mixture was refluxed overnight (Scheme S1-d). The solvent was evaporated under reduced pressure, and residue was dissolved in DCM. Then followed by washing with brine (100 mL) three times and organic layer was dried over anhydrous sodium sulphate and further purified by column chromatography. Recrystallization with DCM/MeOH

gave pure product **1** (brick red solid, yield = 136 mg, 75%). **(1)** ^{1}H NMR (600 MHz, $CDCl_3$): δ (ppm) 8.76 (d, *J* = 4.9 Hz, 4H), 8.70 (d, *J* = 4.9 Hz, 4H), 8.38 (d, *J* = 7.9 Hz, 4H), 8.14 (d, *J* = 7.6 Hz, 4H), 8.11 (d, *J* = 7.9 Hz, 4H), 8.04 (d, *J* = 7.6 Hz, 4H), 4.55 (q, *J* = 7.2 Hz, 4H), 1.53 (t, *J* = 7.2 Hz, 6H), 1.48(s, 24H); ^{13}C NMR (151 MHz, $CDCl_3$)): δ (ppm) 166.87, 145.73, 143.74, 142.81, 142.38, 133.83, 133.40, 133.36, 132.69, 132.06, 130.16, 128.22, 119.50, 118.13, 84.26, 61.41, 25.17, 14.62; UV-vis (CH_2Cl_2): λ/nm (ε/$M^{-1}cm^{-1}$) 416 (184000), and 528 (14000); MALDI-TOF MS *m/z* ([M - e^-]$^{+\cdot}$) 1064.38, calculated for $C_{62}H_{58}B_2N_4NiO_8$:1064.39.

Synthesis of Porphyrin Nanoring

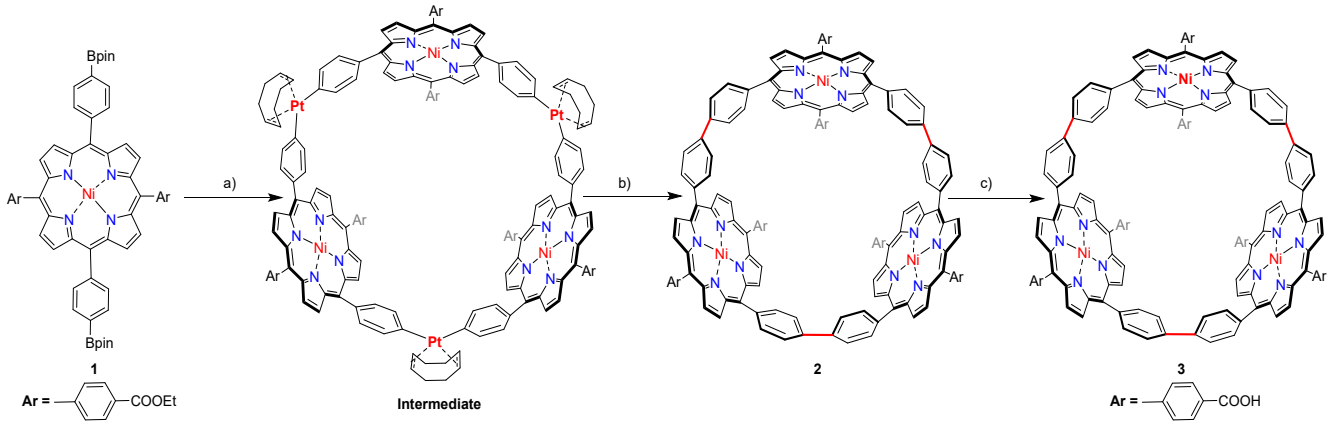

Scheme S2. Synthesis of porphyrin nanorings for HOF, Conditions: **a)** Pt(cod)Cl_2, CsF, THF, reflux; **b)** PPh_3, toluene reflux 2 h; **c)** KOH/H_2O, THF/MeOH, reflux.

Synthesis of 2

Porphyrin precursor **1** (100 mg, 0.094 mmol), Pt (cod)Cl_2 (35.1mg, 0.094 mmol) and CsF (85.36 mg, 0.56 mmol) in THF (20 mL) were refluxed at 64 °C for 24 h under inert atmosphere (Scheme S2-a). The solvent THF was removed under vacuum and the residue was re-dissolved in DCM. The mixture was quickly passed through a short silica plug and solvent was evaporated. The dried residue was added into a two-neck flask followed by addition of triphenylphosphine (245.7 mg, 0.94 mmol). The mixture was purged with argon, charged with anhydrous toluene (30 mL) and refluxed for 2 hrs (Scheme S2-b). After cooling down to room temperature, toluene was removed under vacuum. The residue was dissolved in $CHCl_3$ (50 mL) and washed three times with brine (50 mL). The organic layer was dried with anhydrous sodium sulphate and passed through a short silica gel column to afford a crude mixture, which was further subjected to recycling preparative GPC-HPLC. The product cyclic trimer **2** was collected as a dark-green solution, while the higher cyclic oligomers, n = 4, 5 and 6 could not be purified, most probably attributed to the poor solubility of the larger rings. The recrystallization from $CHCl_3$/MeOH, *n*-heptane gave pure product **2** as a dark greenish black solid (yield = 10 mg, 13%). **(2)** ^{1}H NMR (600 MHz, $CDCl_3$): δ (ppm)

8.94 (d, *J* = 4.9 Hz, 12H), 8.48 (d, *J* = 4.9 Hz, 12H), 8.28 (d, *J* = 7.6 Hz, 12H), 7.92 (d, *J* = 7.6 Hz, 12H), 7.46 (d, *J* = 8.4 Hz, 12H), 7.28 (d, *J* = 8.4 Hz, 12H), 4.51 (q, *J* = 7.2 Hz, 12H), 1.50 (t, *J* = 7.2 Hz, 18H); ^{13}C NMR (151 MHz, $CDCl_3$): δ (ppm) 167.00, 144.81, 141.39, 139.88, 138.93, 138.60, 133.67, 133.45, 133.38, 133.01, 130.30, 128.56, 126.44, 118.53, 116.35, 61.61, 14.80; UV-vis (CH_2Cl_2): λ/nm (ε/$M^{-1}cm^{-1}$) 429 (321000), 532 (19000), 560 (20000), and 600 (10000); MALDI-TOF MS *m/z* ($[M - e^-]^{+\cdot}$) 2436.58, calculated for $C_{150}H_{102}N_{12}Ni_3O_{12}$: 2436.58.

Synthesis of 3

The hydrolysis of ester to acid was done by method as previously reported.[5] To a 10 mL flask porphyrin trimer **2** (20 mg, 0.0082 mmol) and mixture of two solvents, THF and MeOH (2:1), i.e., 5 mL THF and 2.5 mL MeOH were added. Then followed by the addition of KOH aqueous solution (46.1 mg, 0.821 mmol in H_2O (2.5 mL). This mixture was refluxed for 24 h (Scheme S2-c). After reaction completion, the solvent was evaporated. The residue was dissolved in water and carefully acidified to pH=3 with dilute hydrochloric acid (2*N* HCl). The dark greenish black solid was collected by filtration, washed with water several times and dried. The sample was further dispersed in ethanol, and the suspension was sonicated, and centrifuged at speed of 4000 RMP for 15 mins. The ethanol was decanted, and this process was repeated 3 to 4 times. The product was soluble in DMSO, DMF and sparingly soluble in dioxane (black solid, yield = 15 mg, 80%). **(3)** ^{1}H NMR (600 MHz, 1,4-Dioxane-d_8): δ (ppm) 10.56 (s, H), 8.90 (d, *J* = 5.0 Hz, 12H), 8.46 (d, *J* = 5.0 Hz, 12H), 8.24 (d, *J* = 7.6 Hz, 12H), 7.93 (d, *J* = 7.6 Hz, 12H), 7.45 (d, *J* = 8.2 Hz, 12H), 7.27 (d, *J* = 8.2 Hz,12H); MALDI-TOF MS *m/z* ($[M - e^-]^{+\cdot}$) 2268.39, calculated for $C_{138}H_{78}N_{12}Ni_3O_{12}$: 2268.39.

3. NMR, FTIR, Mass Spectrometry, and UV-vis Absorption Spectra

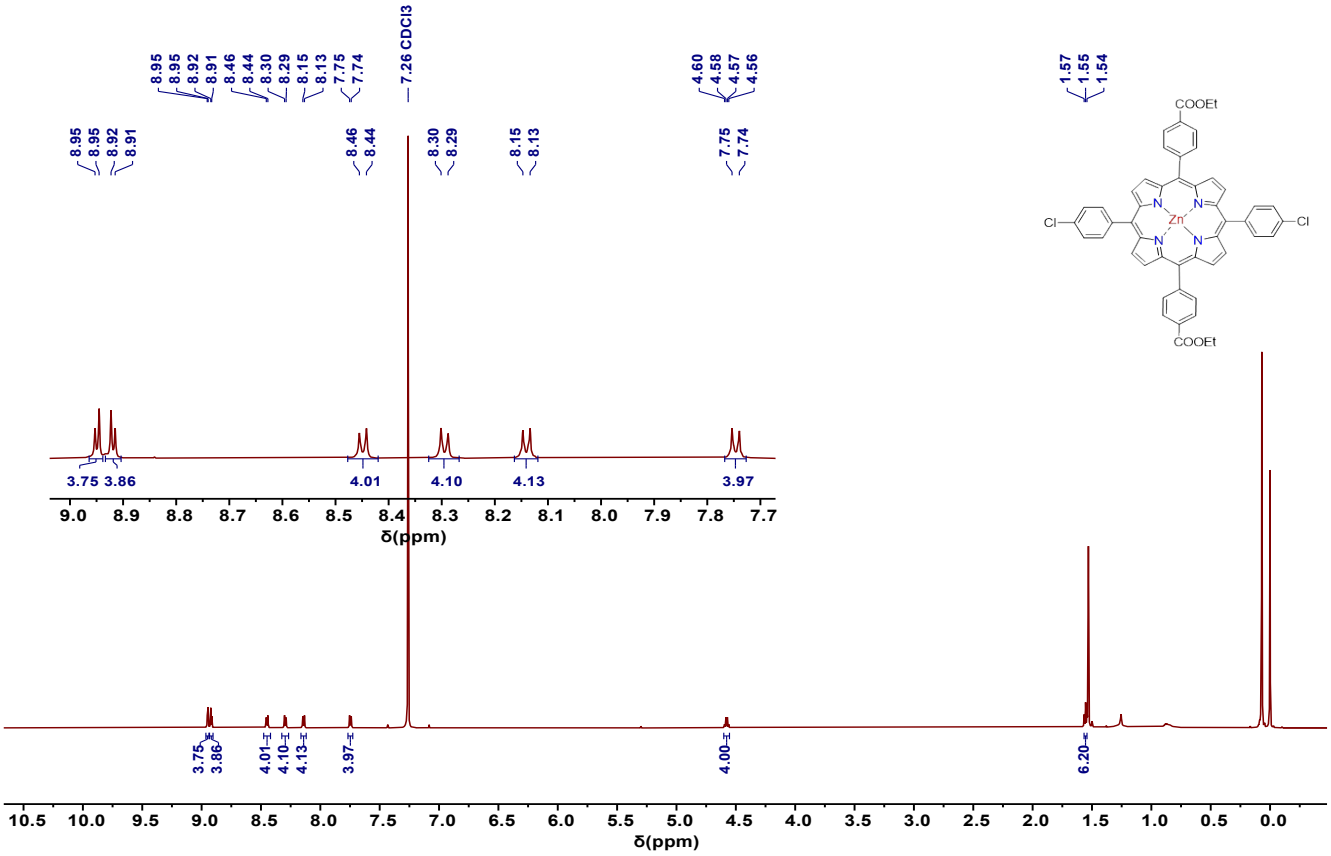

Figure S1. ^{1}H NMR spectrum of **1-Zn-Cl** (600 MHz, $CDCl_3$) at room temperature.

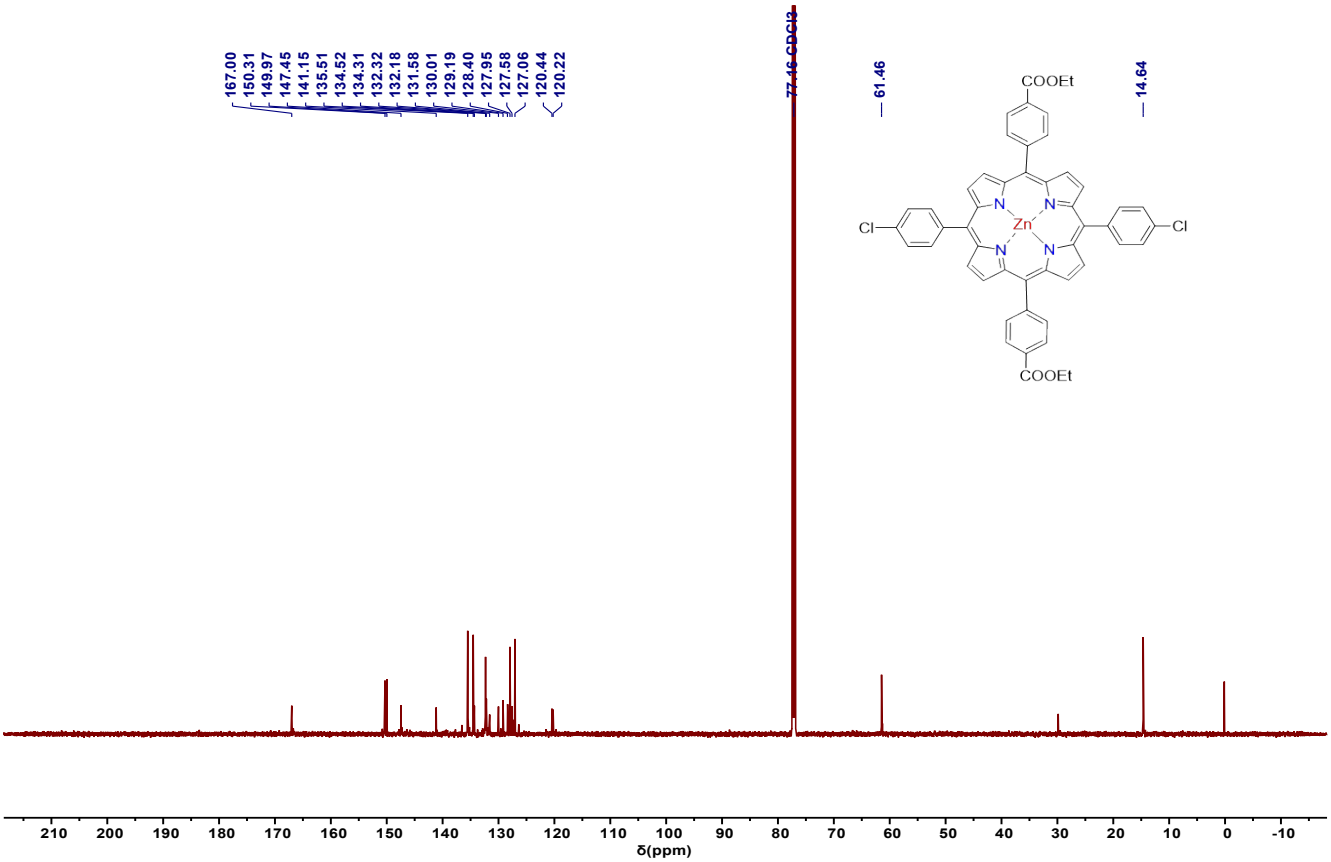

Figure S2. ^{13}C NMR spectrum of **1-Zn-Cl** (600 MHz, $CDCl_3$) at room temperature.

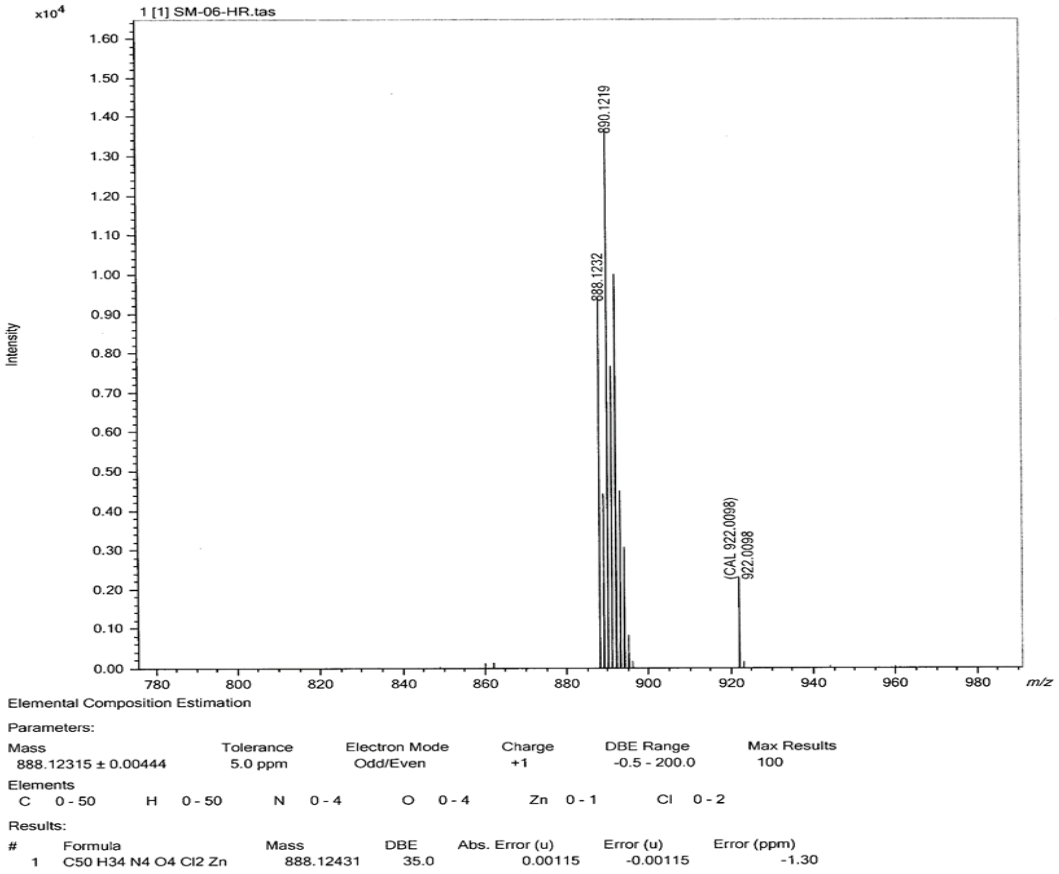

Figure S3. MALDI-TOF MS spectrum of **1-Zn-Cl**.

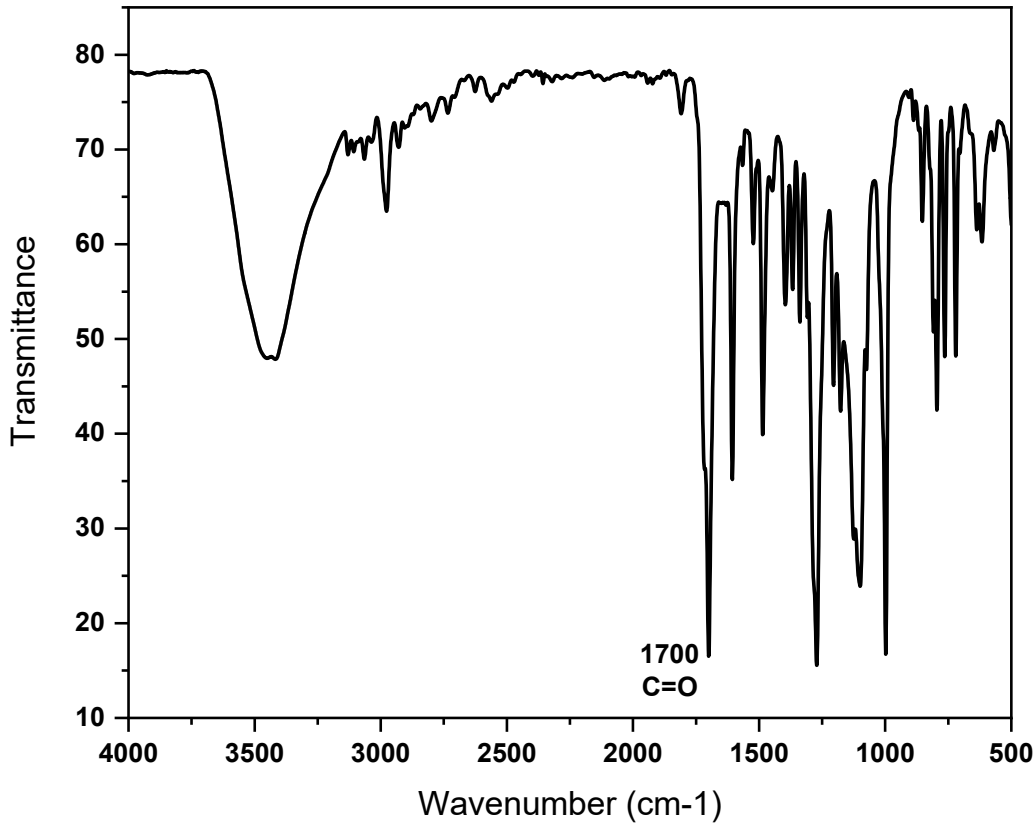

Figure S4. FTIR spectrum of **1-Zn-Cl**.

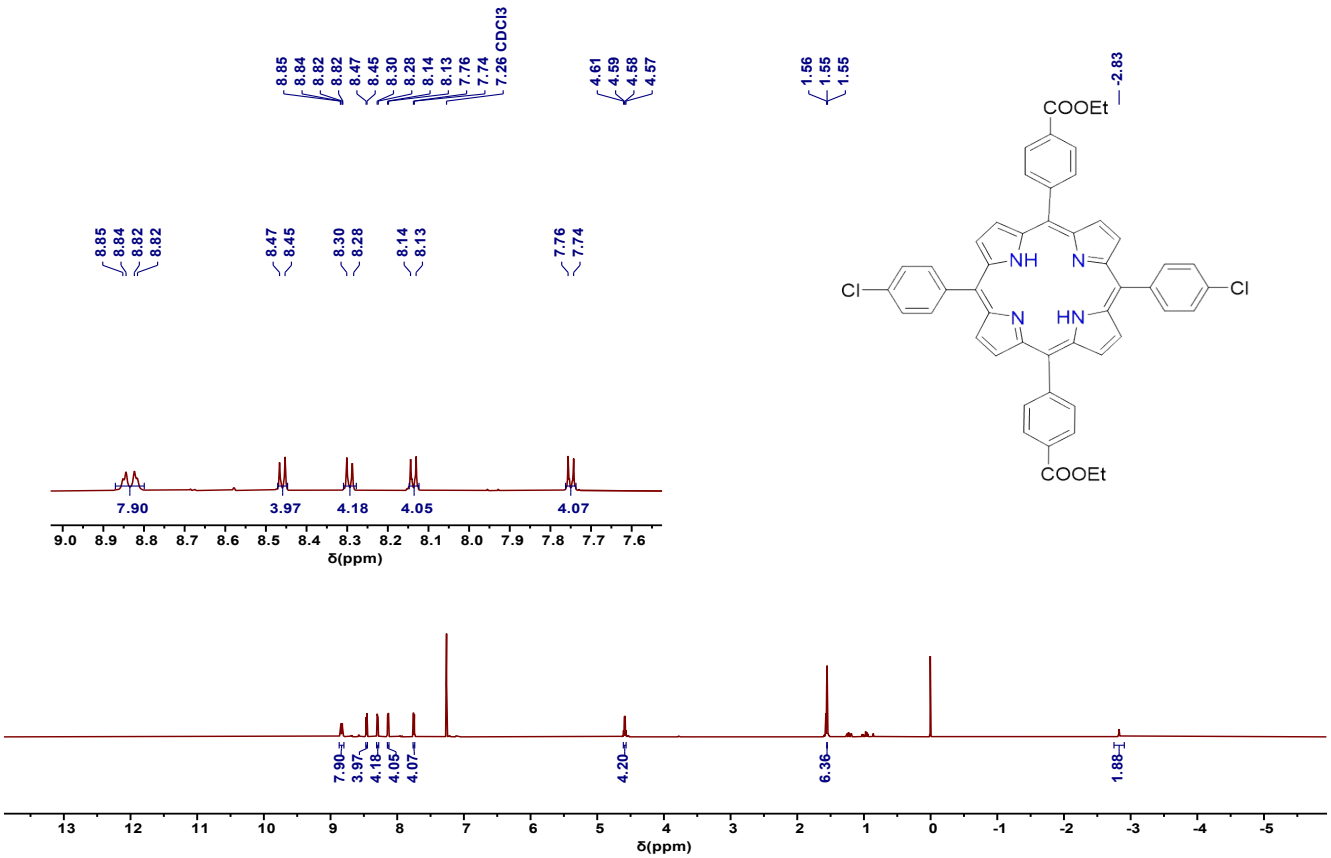

Figure S5. ^{1}H NMR spectrum of **1-H-Cl** (600 MHz, $CDCl_3$) at room temperature.

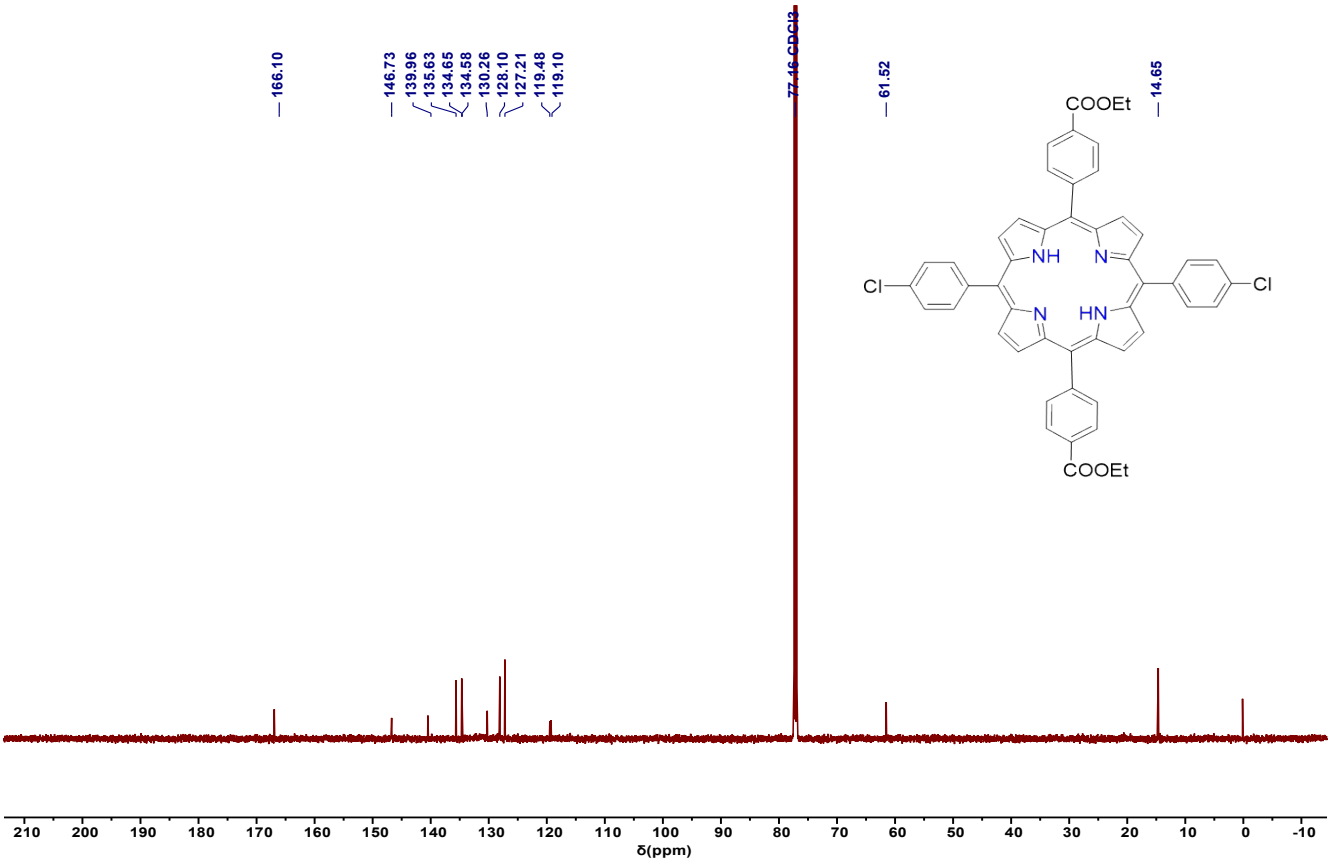

Figure S6. ^{13}C NMR spectrum of **1-H-Cl** (600 MHz, $CDCl_3$) at room temperature.

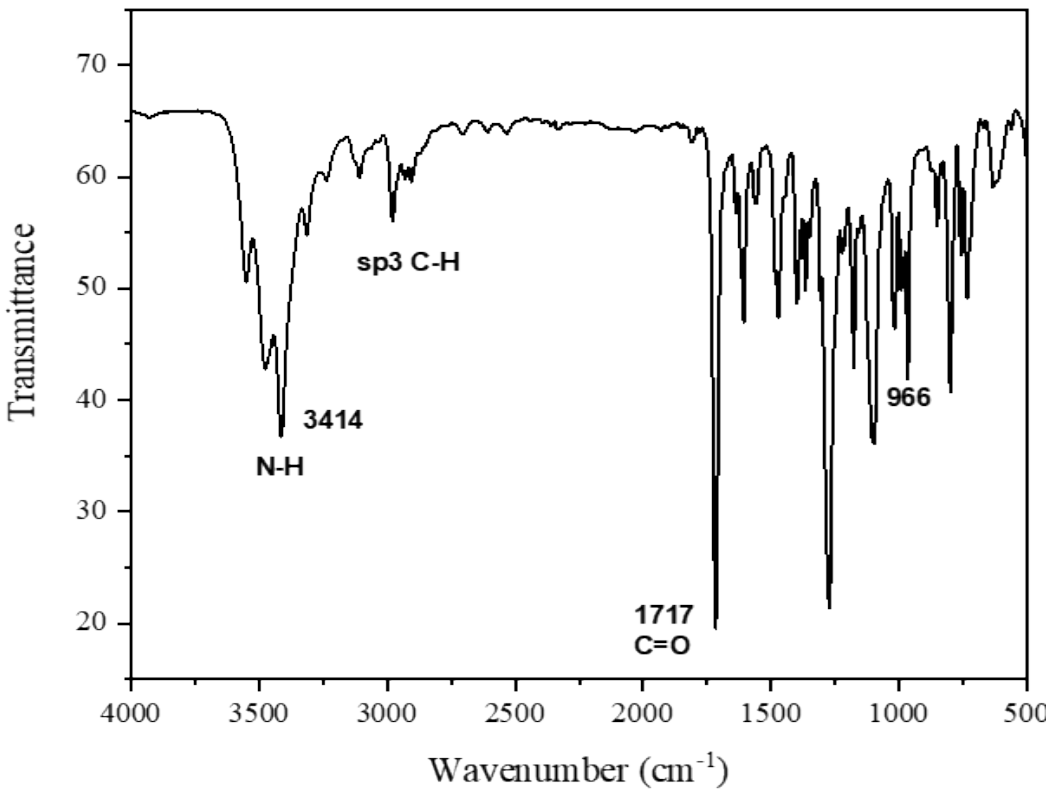

Figure S7. FTIR spectrum of **1-H-Cl**.

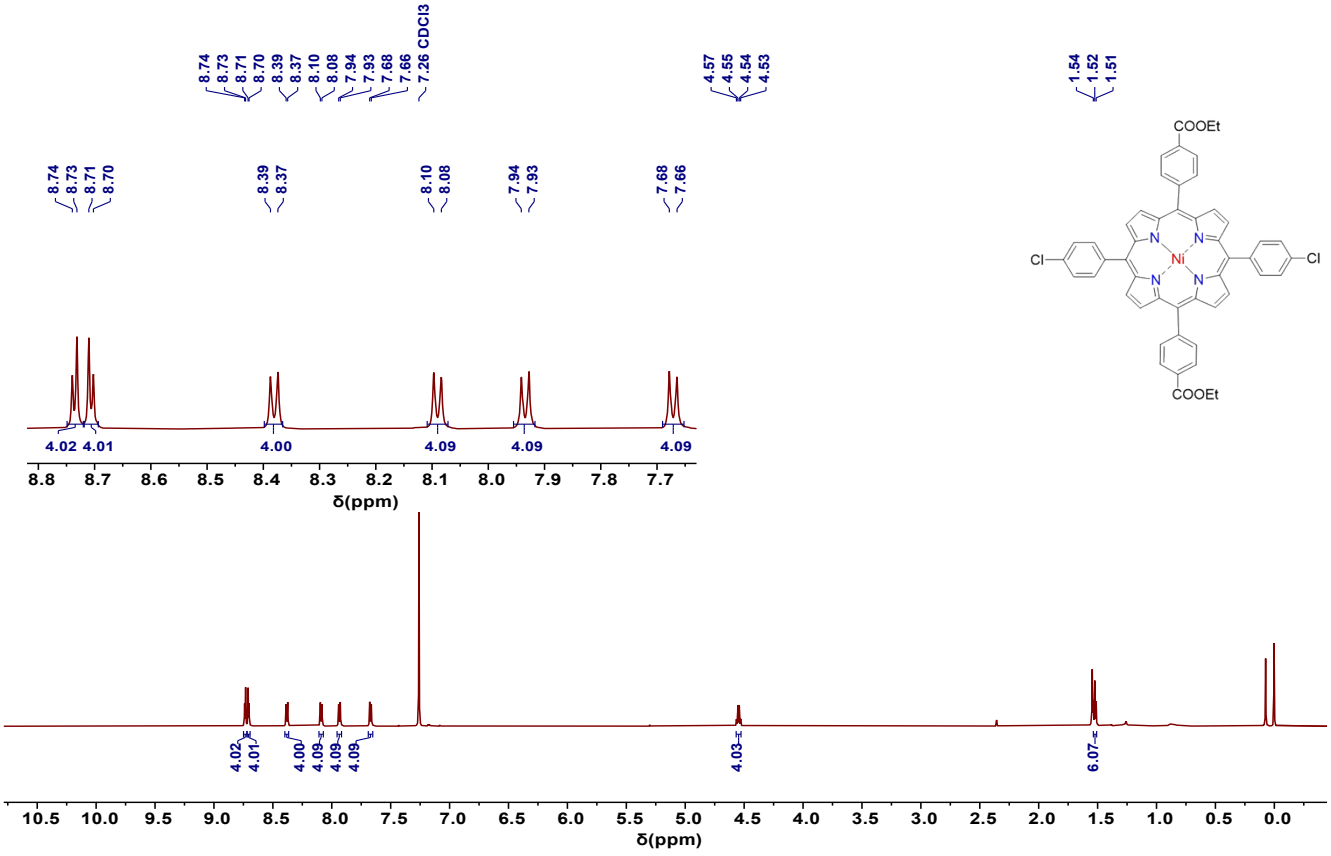

Figure S8. ^{1}H NMR spectrum of **1-Ni-Cl** (600 MHz, $CDCl_3$) at room temperature.

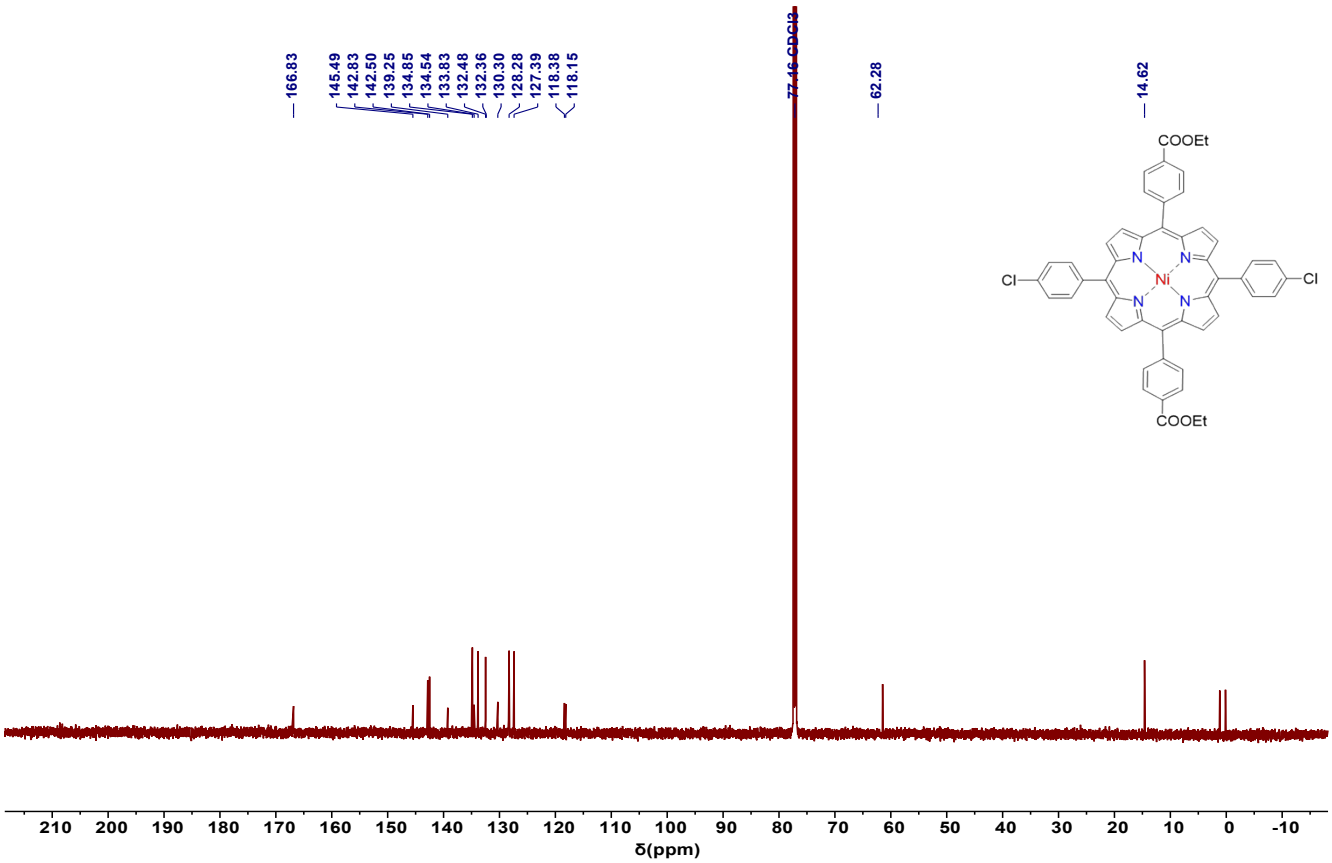

Figure S9. ^{13}C NMR spectrum of **1-Ni-Cl** (151 MHz, $CDCl_3$) at room temperature.

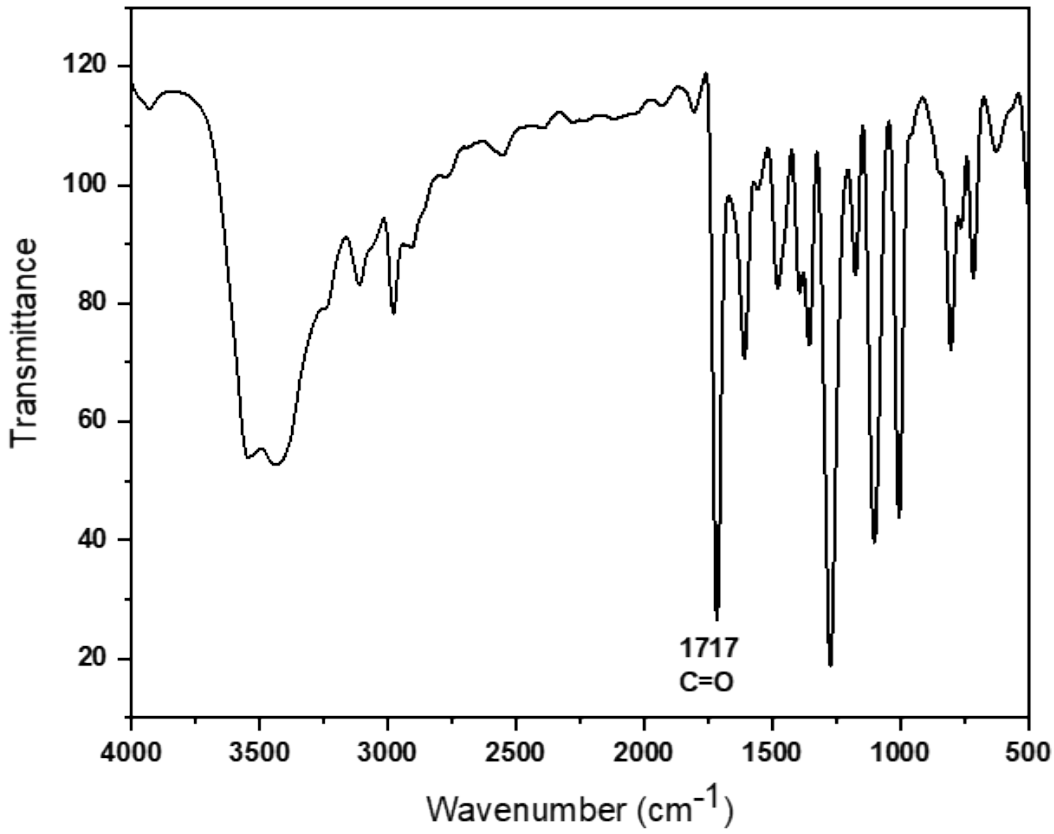

Figure S10. FTIR spectrum of **1-Ni-Cl**.

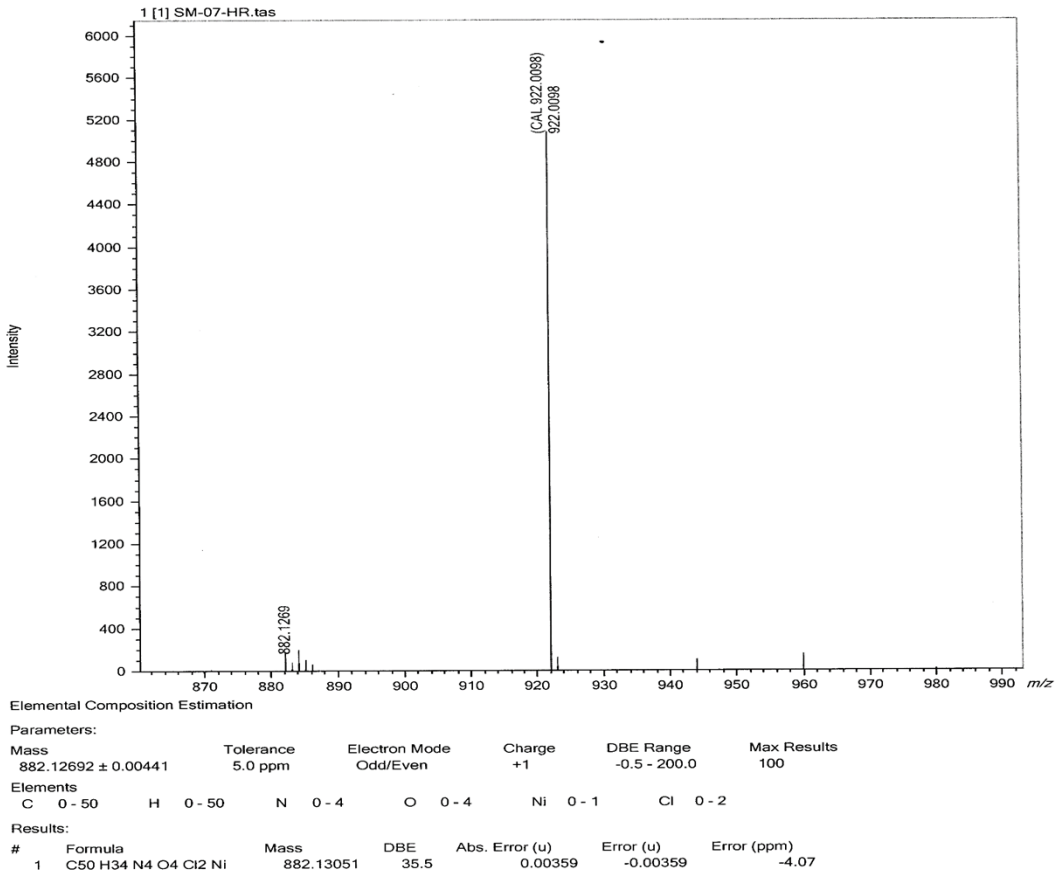

Figure S11. MALDI-TOF MS spectrum of **1-Ni-Cl**.

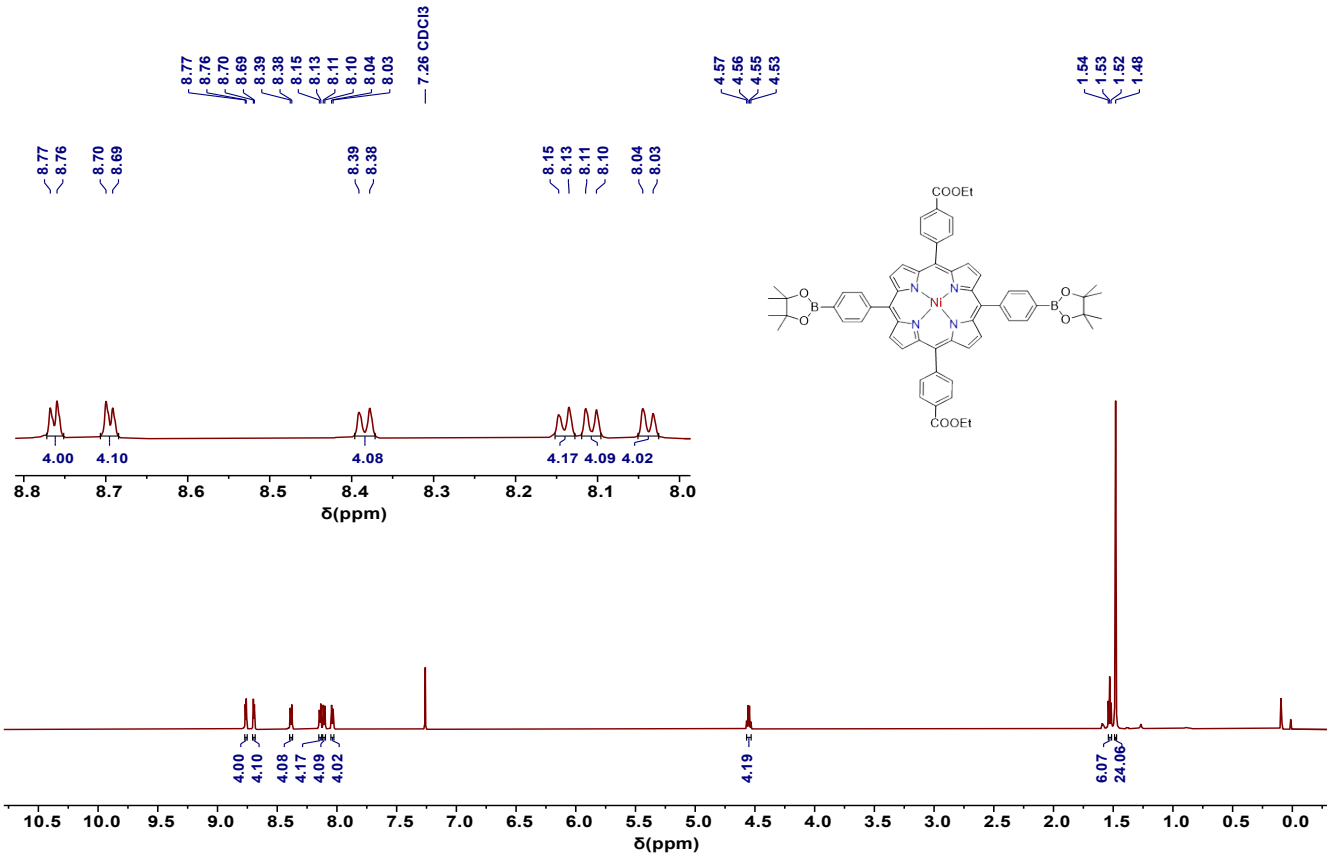

Figure S12. ^{1}H NMR spectrum of **1** (600 MHz, $CDCl_3$) at room temperature.

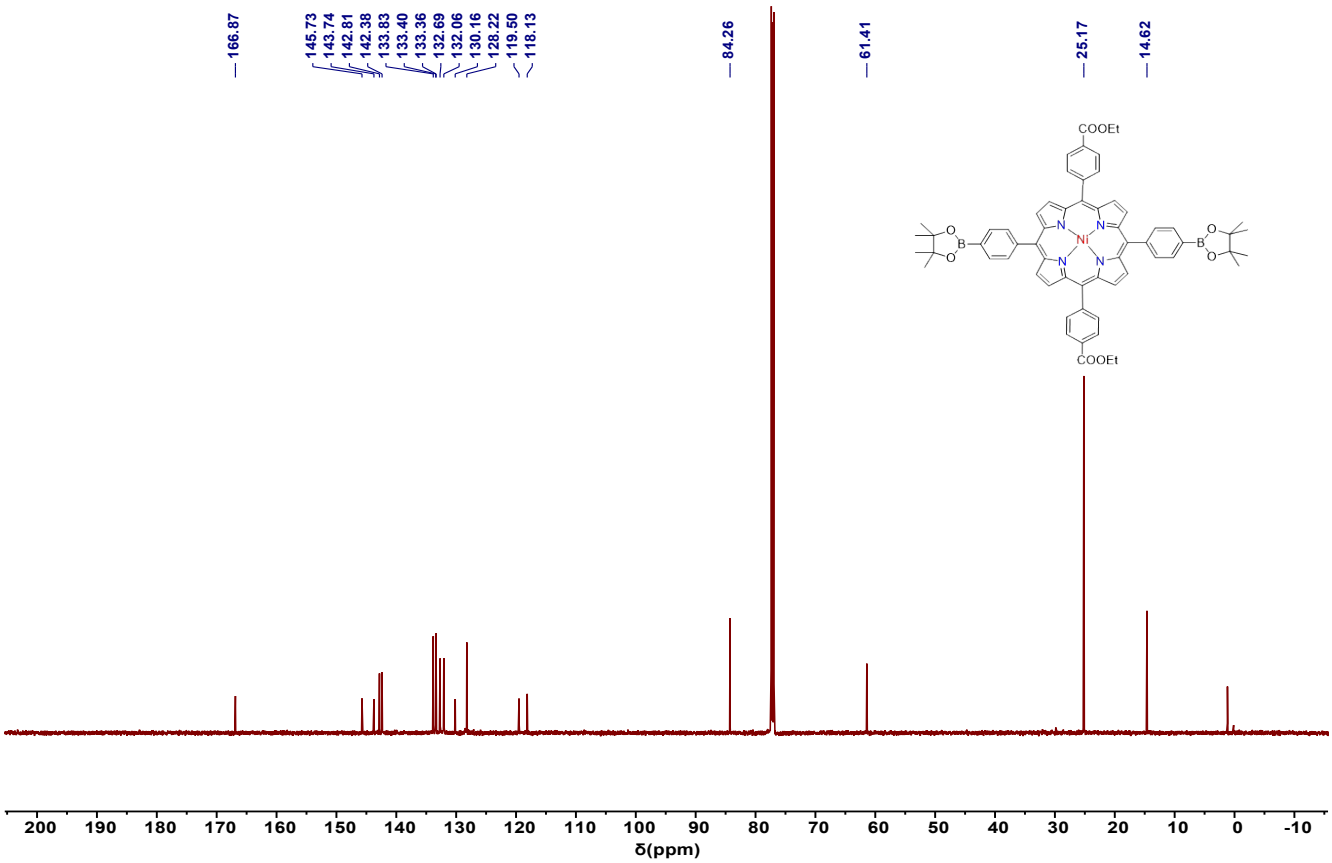

Figure S13. ^{13}C NMR spectrum of **1** (151 MHz, $CDCl_3$) at room temperature.

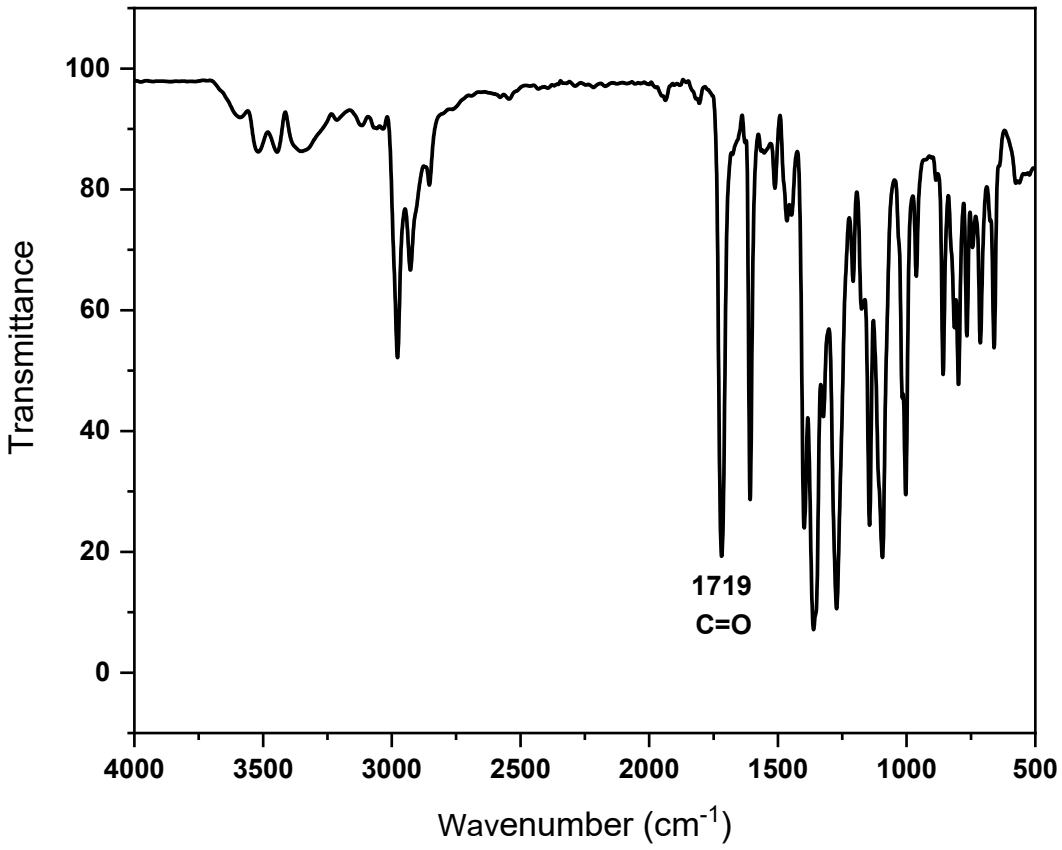

Figure S14. FTIR spectrum of **1**.

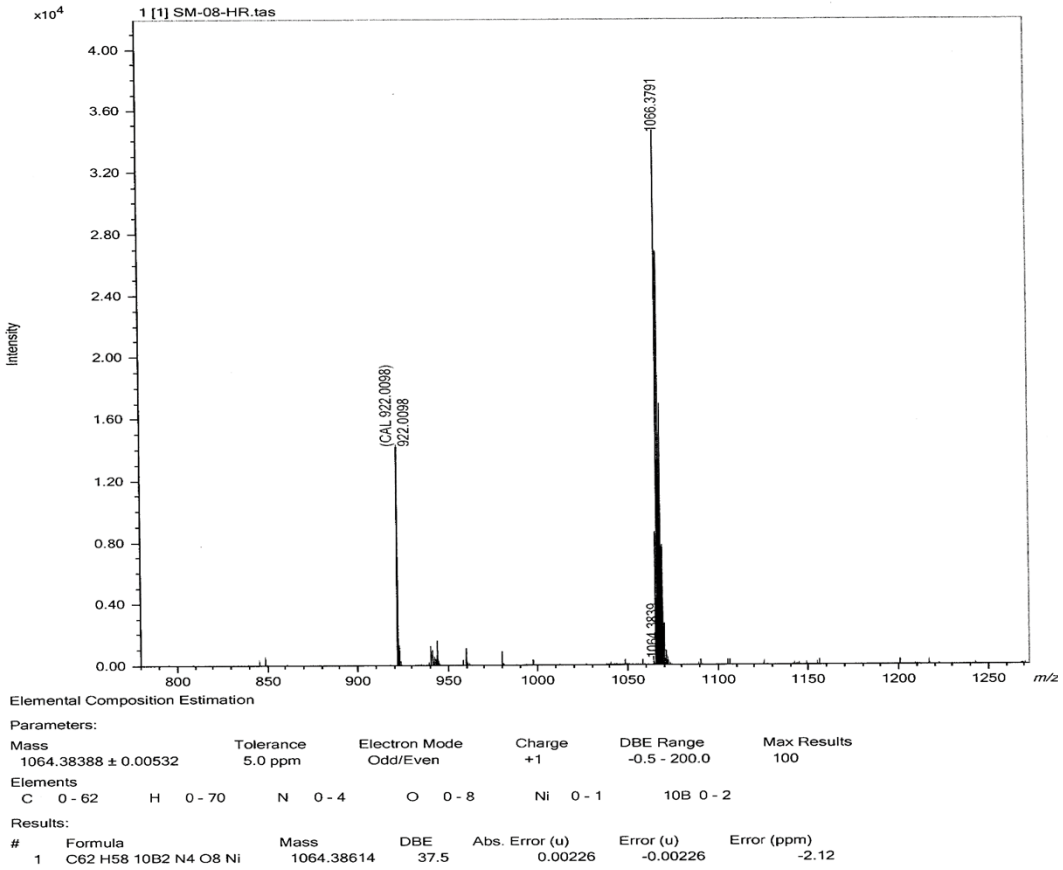

Figure S15. MALDI-TOF MS spectrum of **1**.

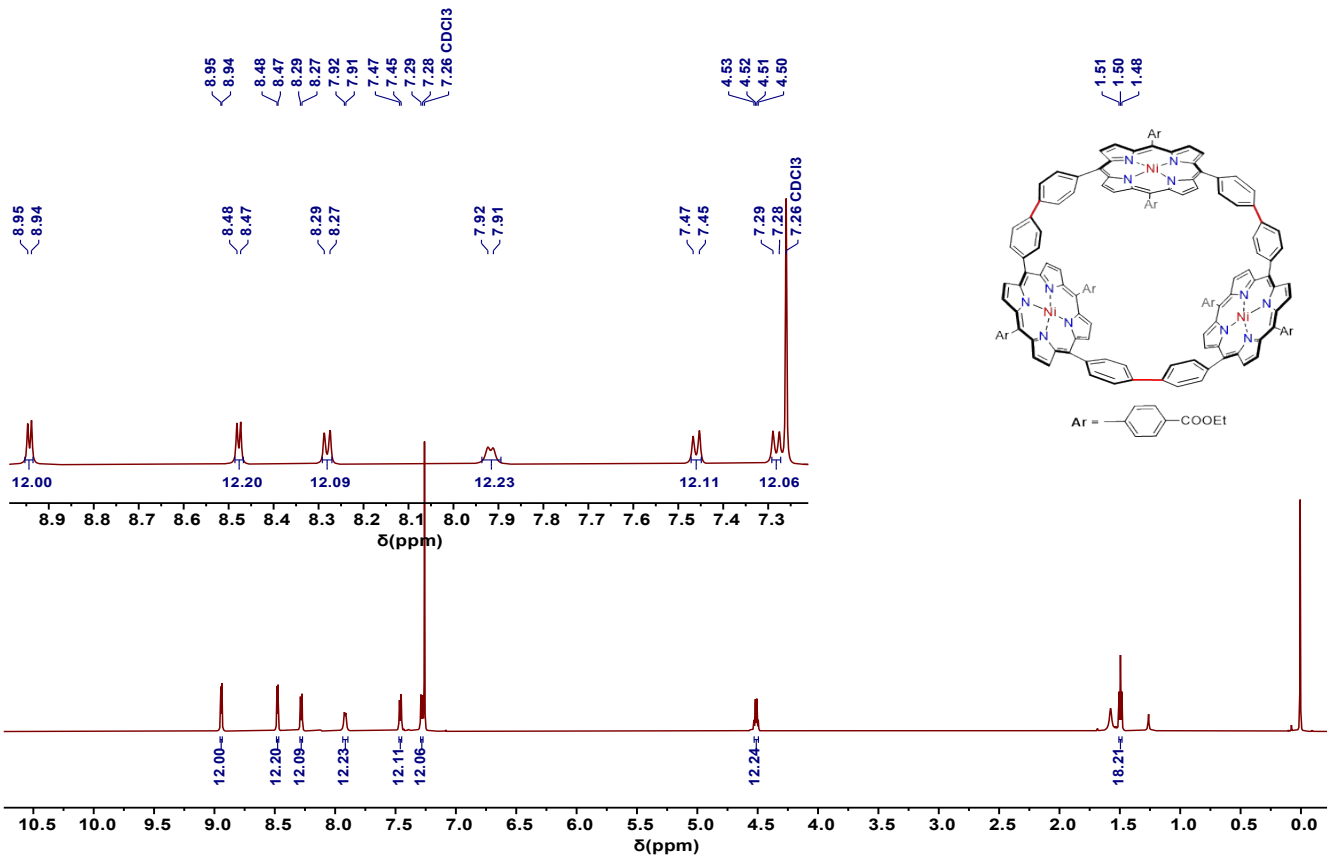

Figure S16. ^{1}H NMR spectrum of **2** (600 MHz, $CDCl_3$) at room temperature.

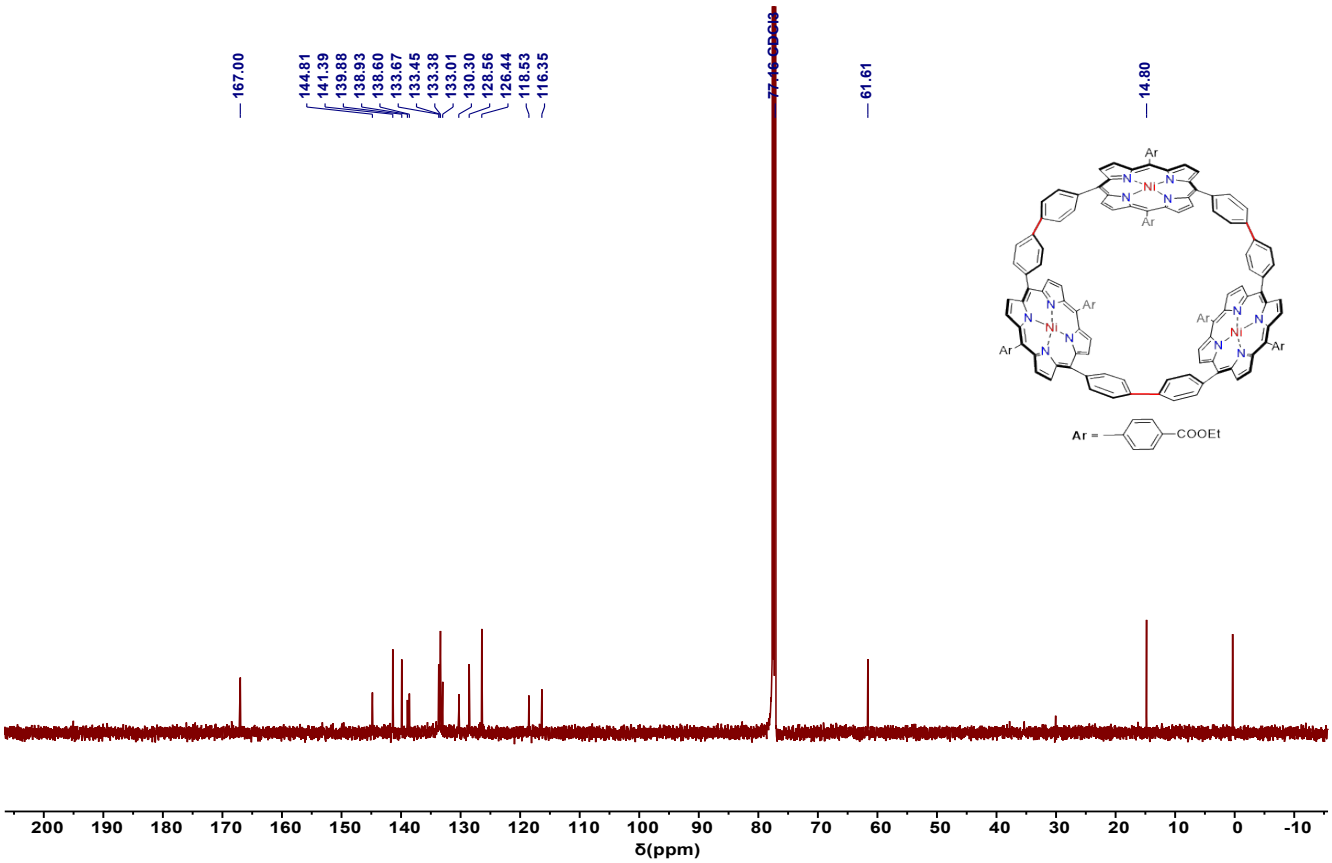

Figure S17. ^{13}C NMR spectrum of **2** (151 MHz, $CDCl_3$) at room temperature.

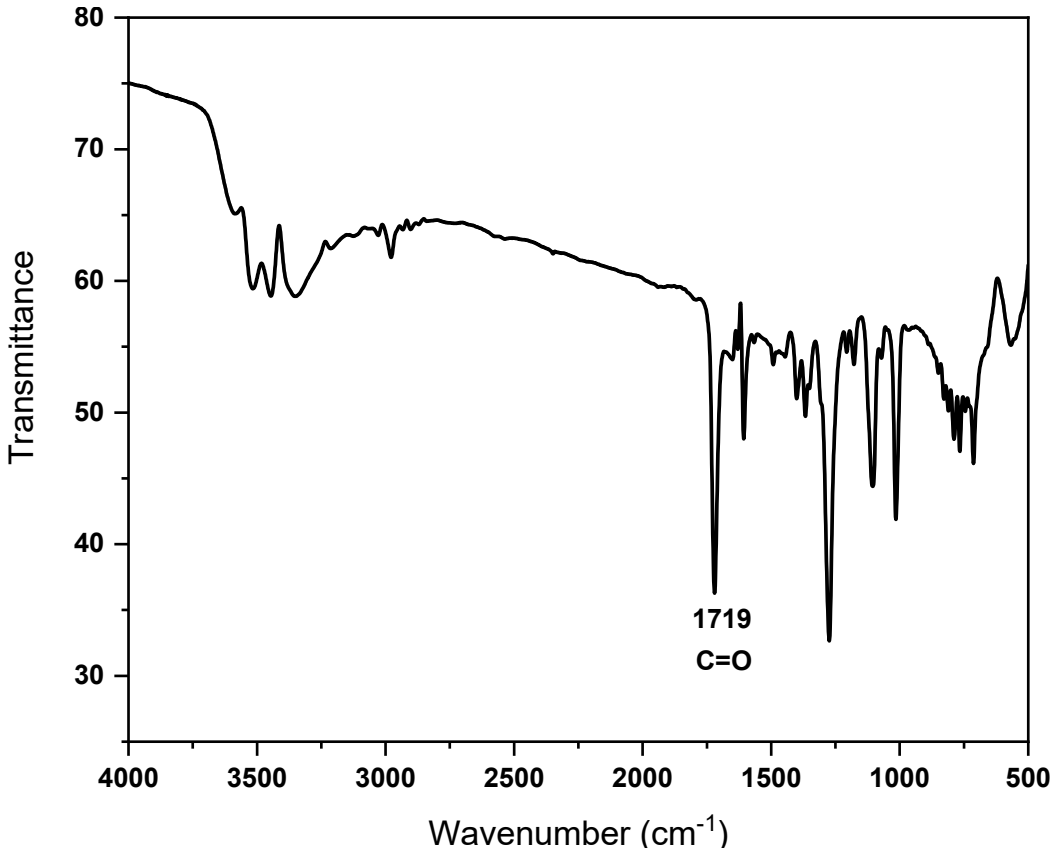

Figure S18. FTIR spectrum of **2**.

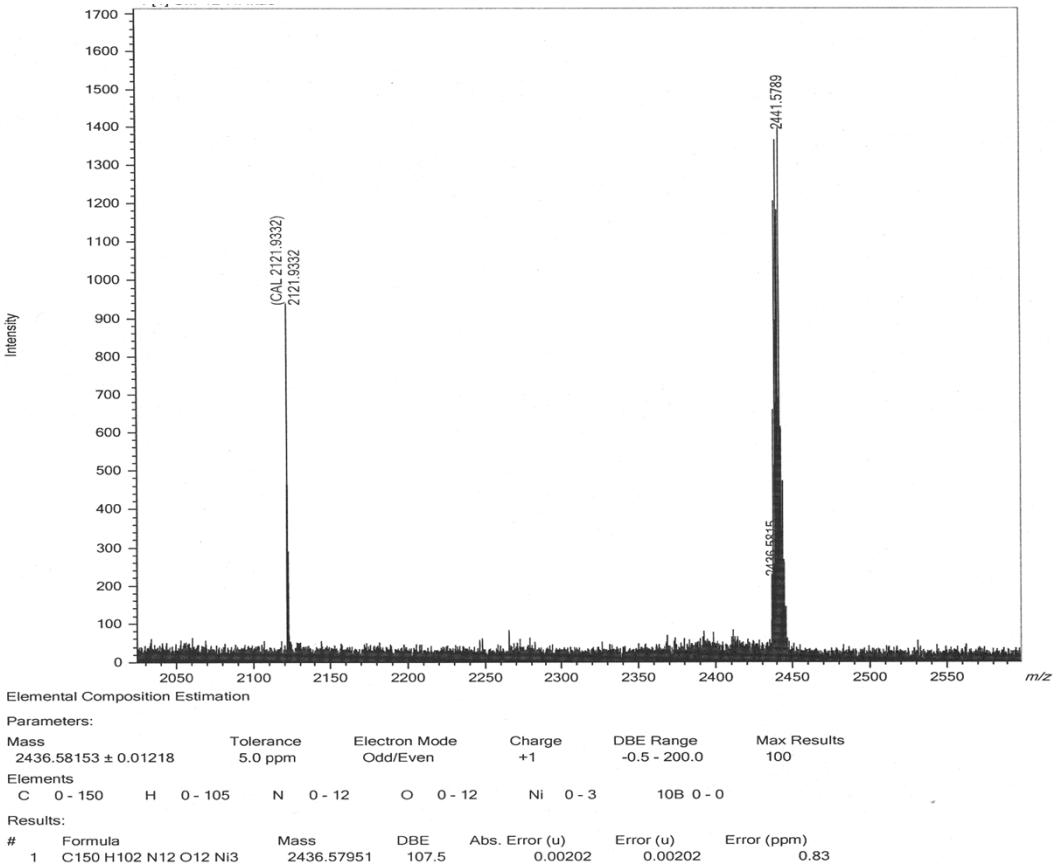

Figure S19. MALDI-TOF MS spectrum of **2**.

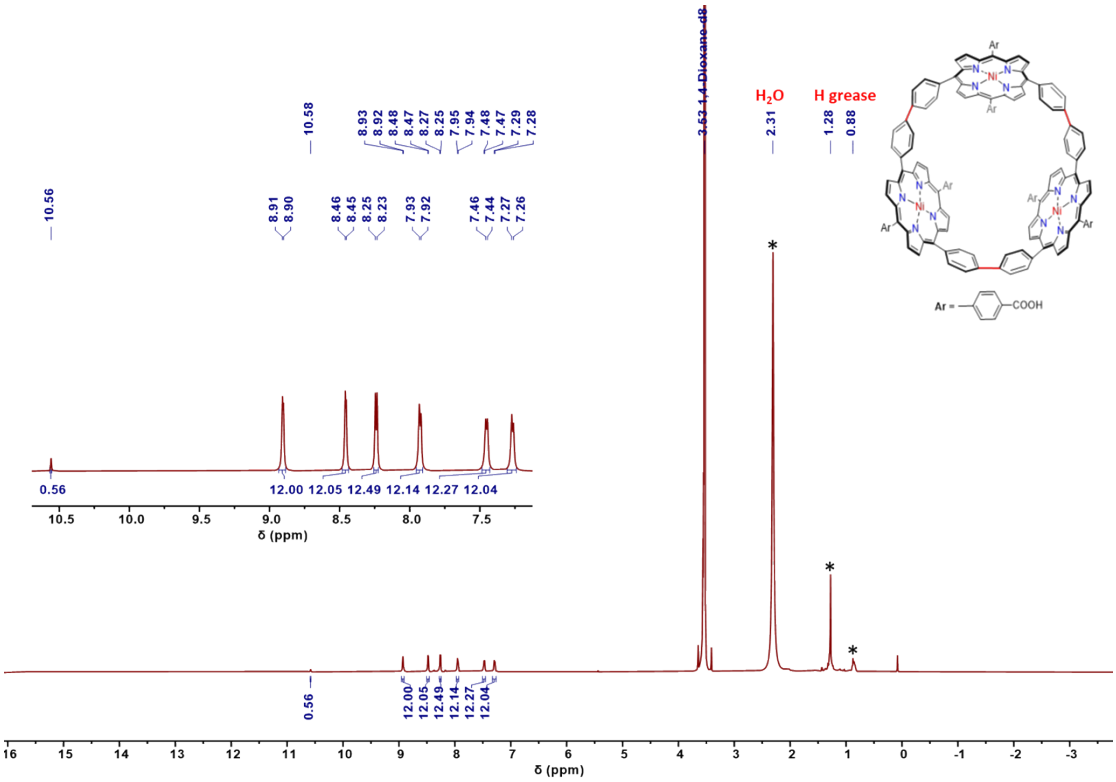

Figure S20. ^{1}H NMR spectrum of **3** (600 MHz, 1,4-Dioxane-d_8) at 60 °C.

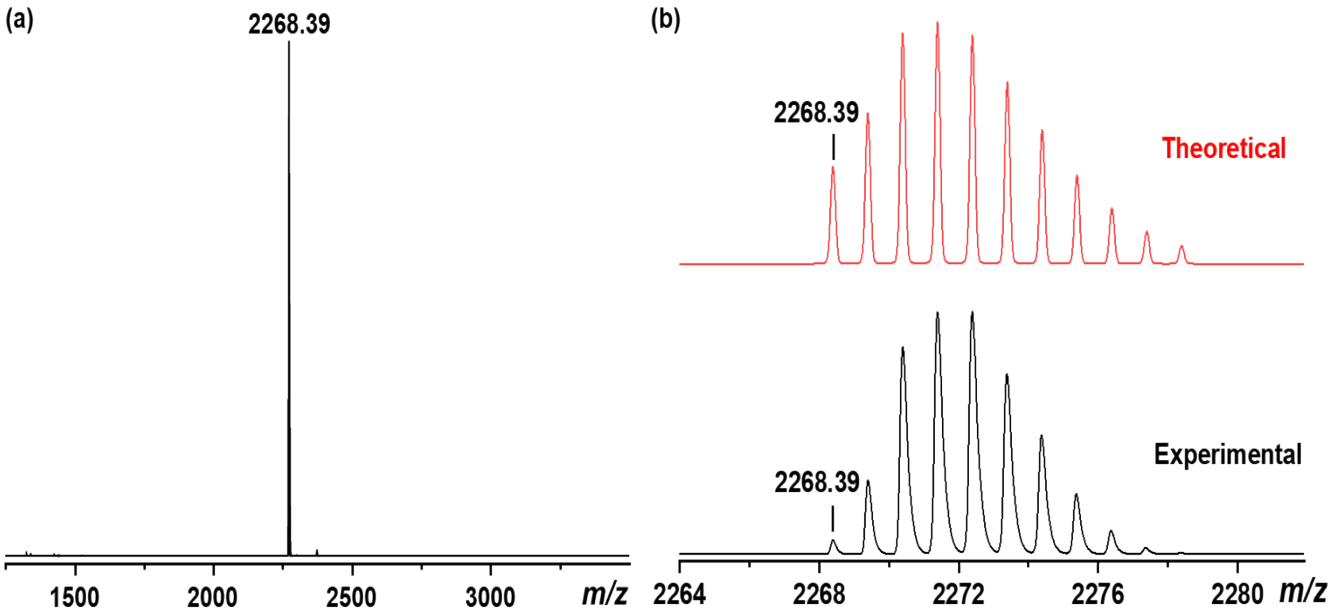

Figure S21. (a) MALDI-TOF MS spectrum of **3** in reflectron positive mode, **(b)** the corresponding experimental and theoretical isotope patterns.

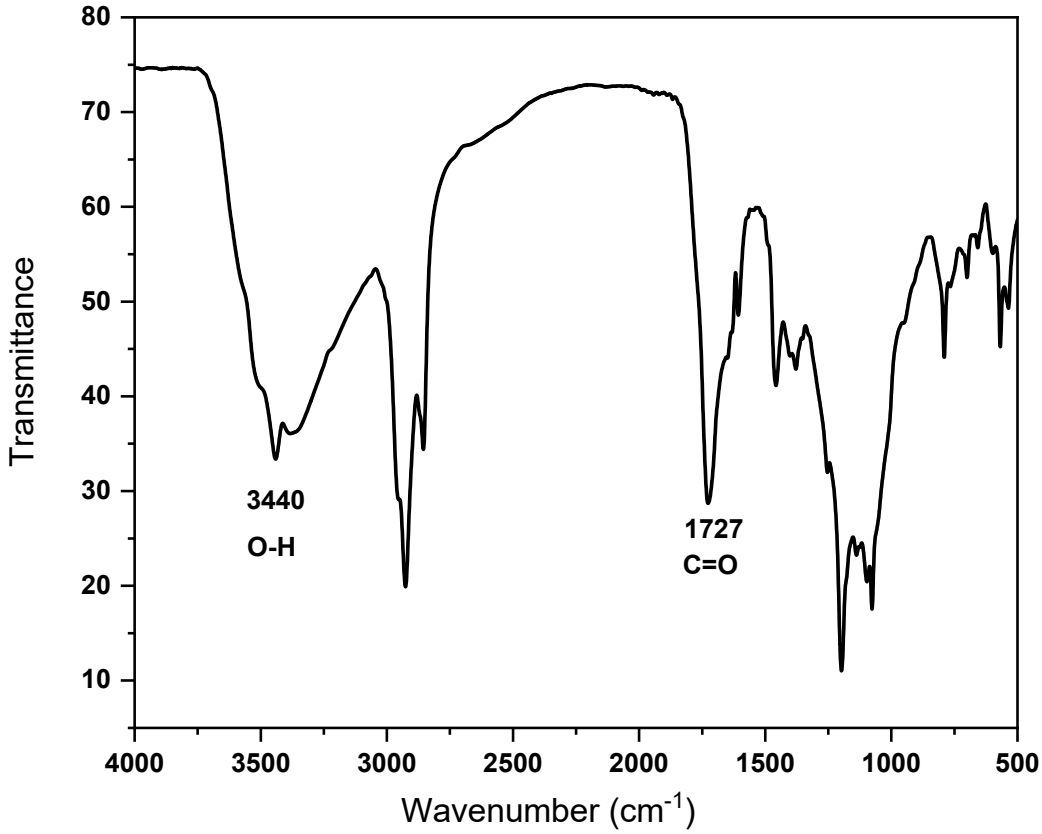

Figure S22. FTIR spectrum of **3**.

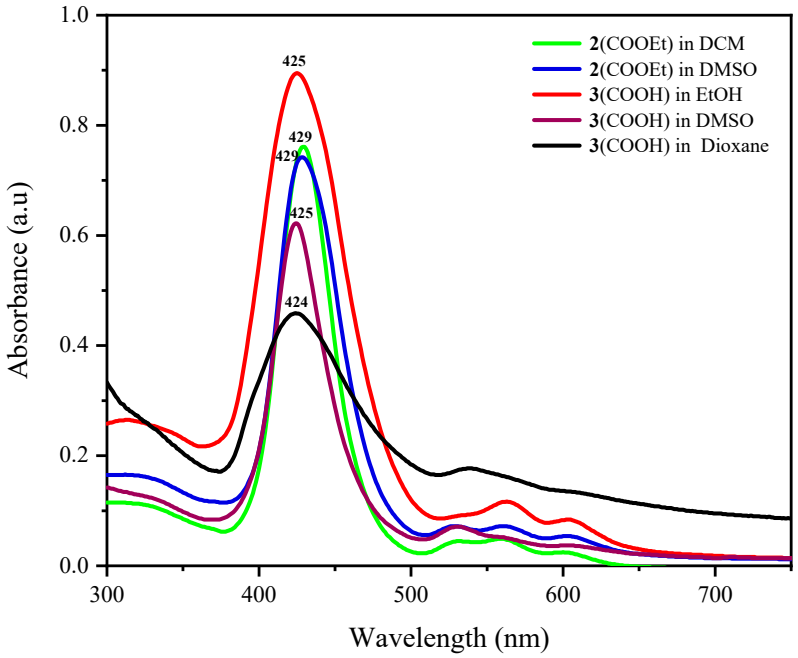

Figure S23. UV-vis absorption spectra of **2** (ester) and **3** (acid) in different solvents at room temperature.

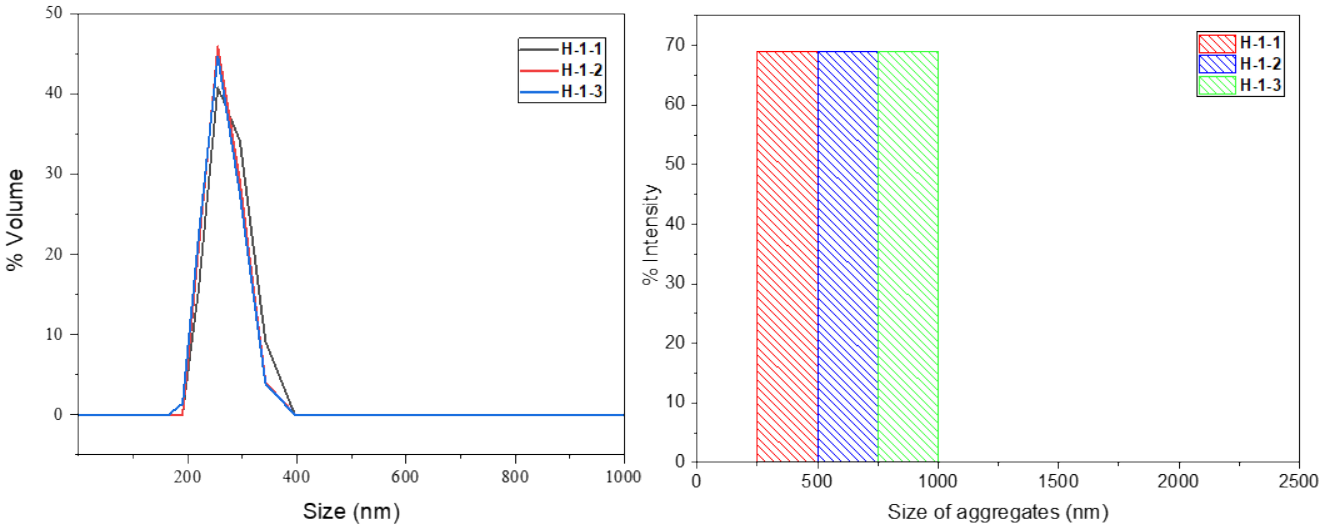

Figure S24. The DLS intensity plots for size distribution of **3** in EtOH.

The PNRs **3** (0.3 mg) was added to 3 mL EtOH in a glass vial and the mixture was sonicated and used for dynamic light scattering (DLS) measurements. The sample was analyzed three times and the peaks observed in Figure S24 suggested that the self-assembly of **3** can occur in solution phase as well. Hence in EtOH suspension of **3,** one dimensional stacking of **3** were observed indicated that the self-assembly of PNRs **3** via H-bonding between carboxylic groups. DLS measurements were found to give results consistent with MALDI TOF and UV-visible absorption of the 1D self-assembly of PNRs **3** towards PNTs.

4. SEM measurements

The sample for SEM measurements was prepared by slow aggregation process to achieve long range ordered self-assembly of porphyrin nanorings (PNRs) to porphyrin nanotubes (PNTs). First, PNRs **3** (0.4 mg) was added to 0.2 mL of 1,4-dioxane in a 1 mL glass vial. The mixture was sonicated then put in another comparatively bigger glass vial containing toluene (0.3 mL) and left it for aggregation overnight at room temperature with slow evaporation of toluene. The SEM images from above solution were obtained by drop-casted on silicon substrate. The solvents were evaporated under heating lamp about 50 °C, followed by platinum coating. On large area long 1D nanostructures were observed. The morphology of the sample demonstrated that porphyrin macrocycles had self-assembled into long tubular framework. In this case, the length of PNTs increased to large extent up to several micrometers but the tubes were entangled with each other as shown in SEM images (Figure S25).

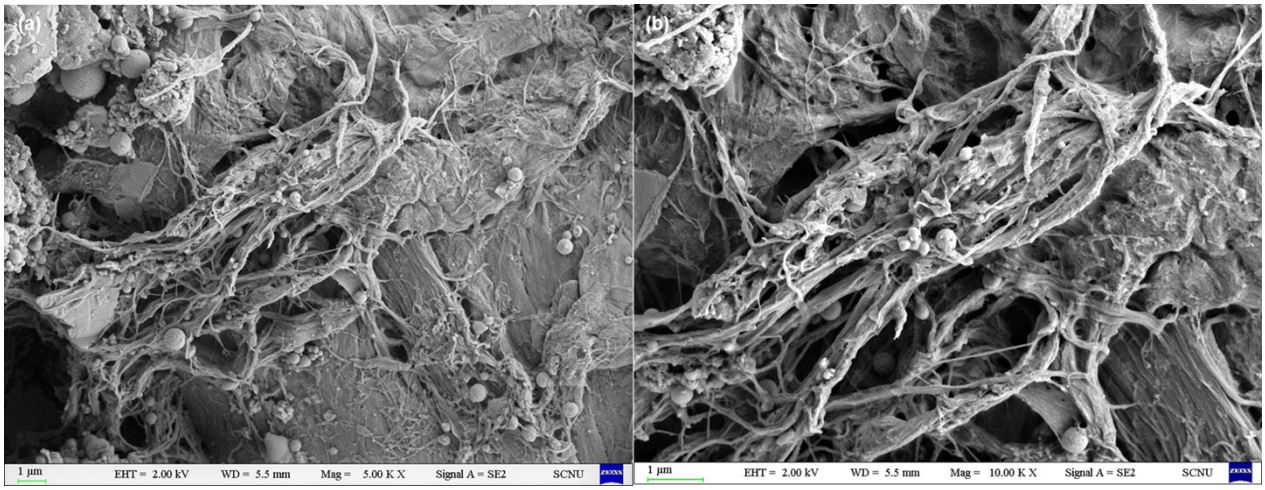

Figure S25. (a-b) SEM images of porphyrin nanotubes suspension in dioxane/toluene adsorbed on silicon substrate indicating bundles of several tightly packed nanotubes.

As some spherical structures were observed in above micrograph, we speculated that they might be salt residues. To remove such residues from the product, a suspension of **3** in ethanol was prepared by sonication and then followed by centrifugation for 15 mins at 4000 rpm. Ethanol was decanted and this process was repeated three times. 1,4-dioxane (0.2 mL) was added to the dried sample of **3** (0.4 mg) in a 1 mL glass vial. Then sonicated it for long time until it was completely dissolved. The sample was left overnight at room temperature for aggregation in a capped glass vial without slow evaporation of toluene. For SEM imaging, a small drop of the prepared sample was taken on silicon substrate without further dilution (Figure S26). The images show that PNTs are several micrometers long but still packed in the form of bundles. These PNTs, upon sonication got disassembled as observed by SEM (Figure S27). When the resulting suspension was left overnight at room temperature, they regenerated again to form 1D PNTs designating the reversibility of this self-assembly process.

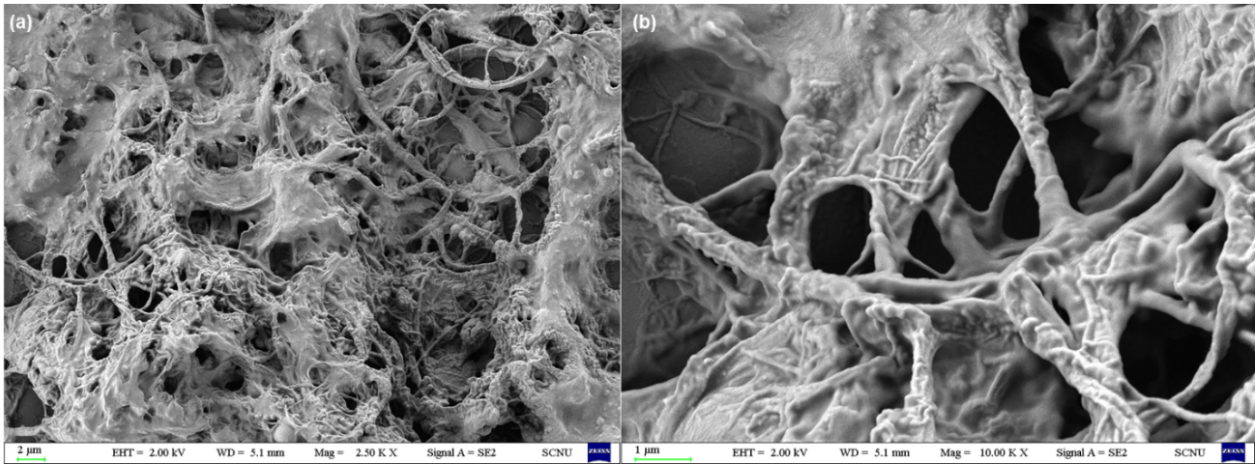

Figure S26. (a-b) SEM images of porphyrin nanotubes suspension in only dioxane adsorbed on silicon substrate indicating bundles of several tightly packed nanotubes.

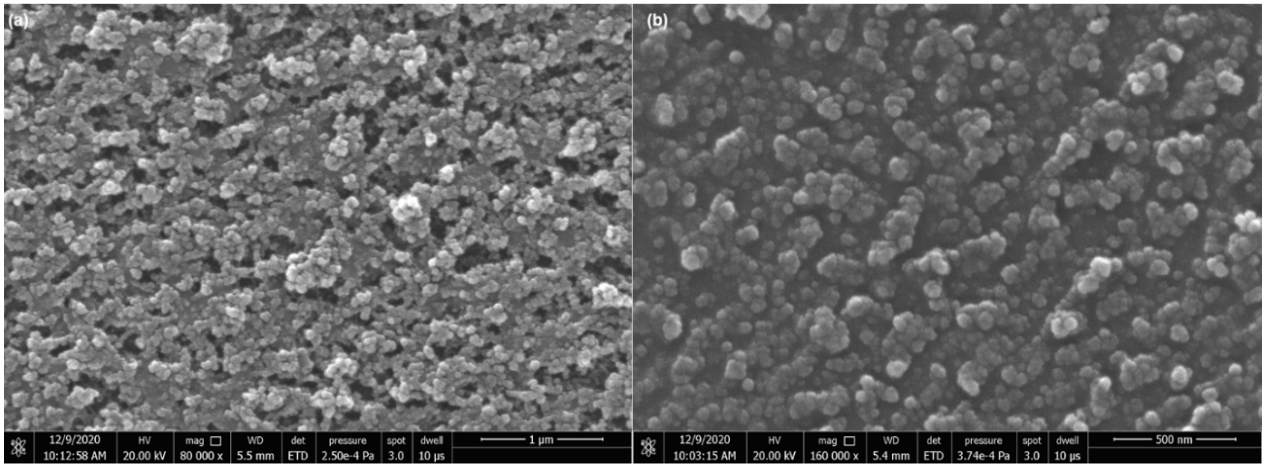

Figure S27. (a-b) SEM images of PNTs suspension in dioxane/toluene after sonication.

The de-bundling of PNTs was achieved by addition of toluene (2 mL) to the same sample in Figure S26, toluene enabled the PNTs to get dispersed from each other as shown in the images (Figure S28).

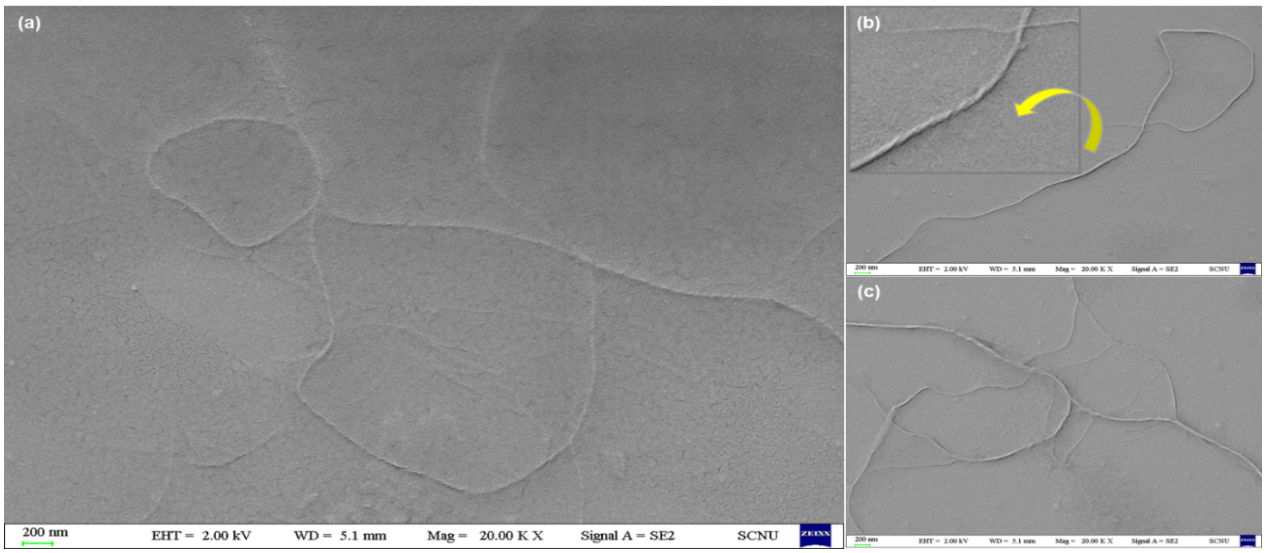

Figure S28. (a-c) SEM images of PNTs dispersed in toluene adsorbed on silicon substrate indicating spiral (rope- like) packing.

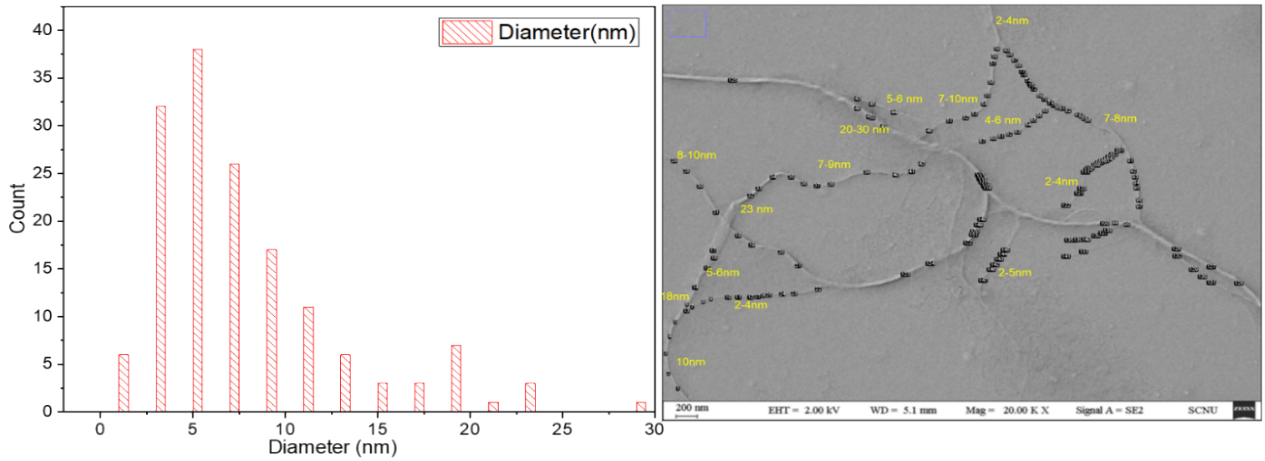

Figure S29. Histogram for diameter estimation of PNTs bundles with respective micrograph of PNTs.

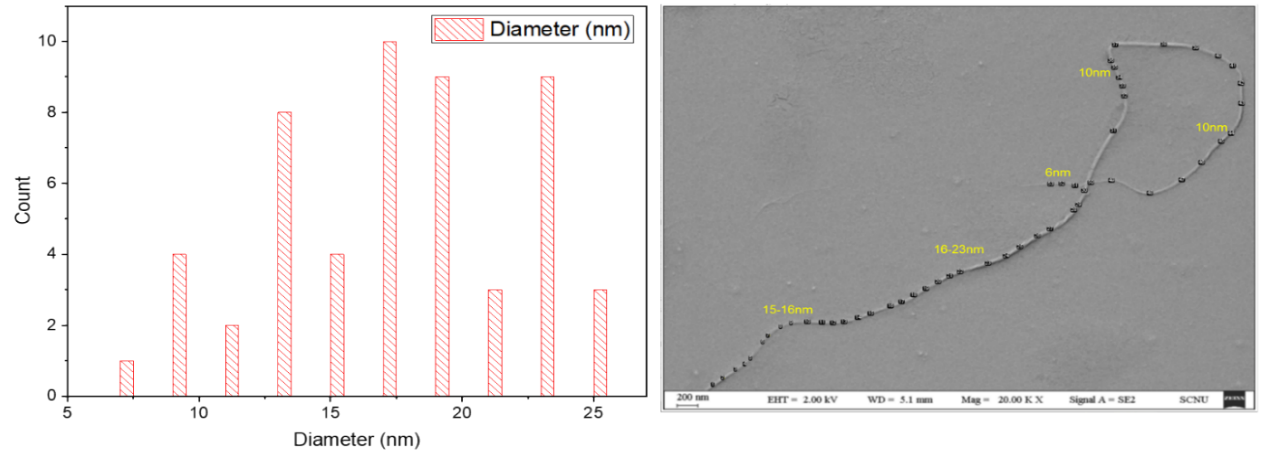

Figure S30. Histogram for diameter estimation of PNTs bundles with respective micrograph of PNTs.

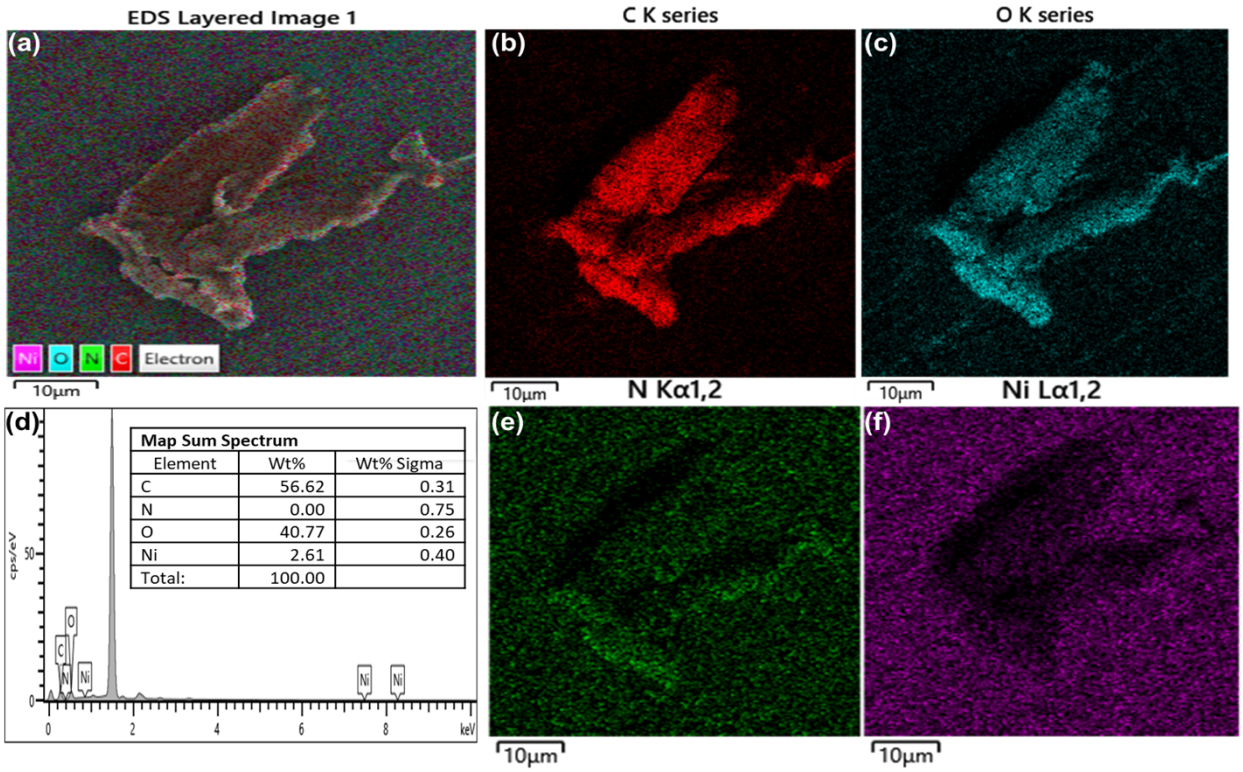

Figure S31. EDS mapping of PNTs **(a)** is corresponding image **(b)** C, **(c)** O, **(e)** N, **(f)** Ni are elements. **(d)** EDX spectrum.

5. TEM Measurements

The transmission electron microscope (TEM) further confirmed the formation of hollow tubular morphology of PNTs.

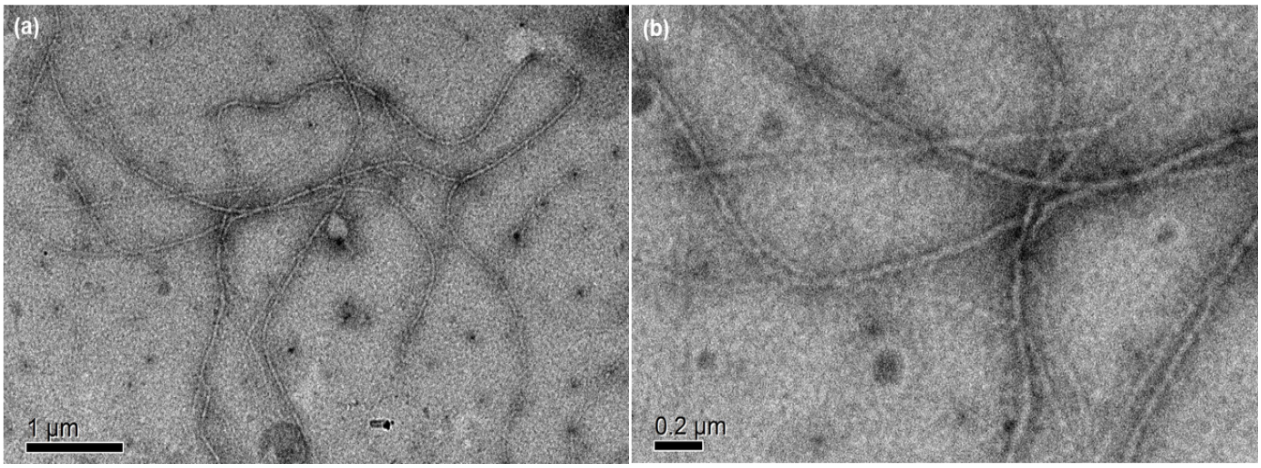

Figure S32. (a-b) 120 kV JEM-1400 PLUS TEM, micrographs of PNTs suspension in dioxane/toluene.

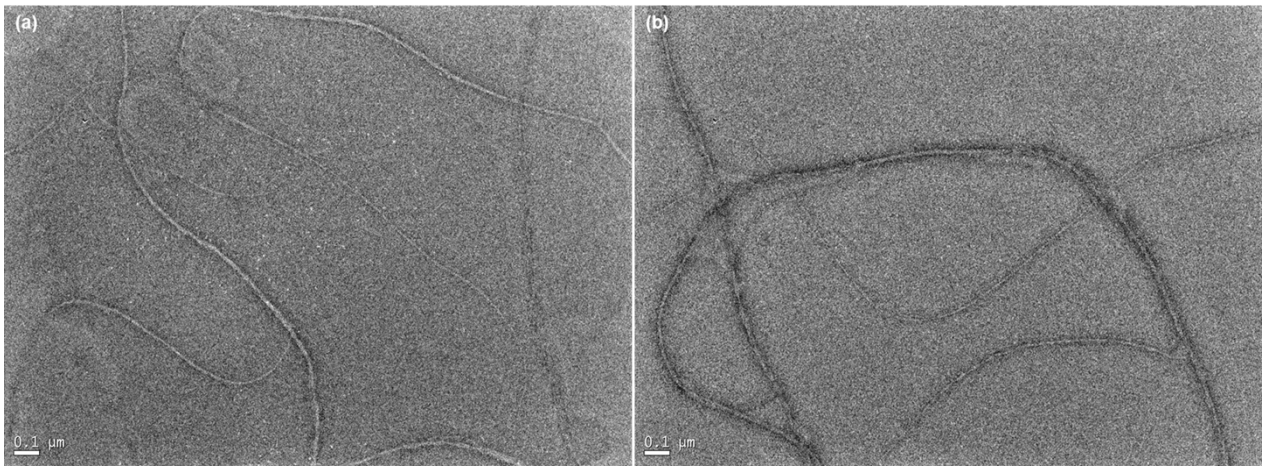

Figure S33. (a-b) 200 kV JEM-2100HR TEM, micrograph of PNTs suspension in dioxane/toluene placed on ultrathin carbon film.

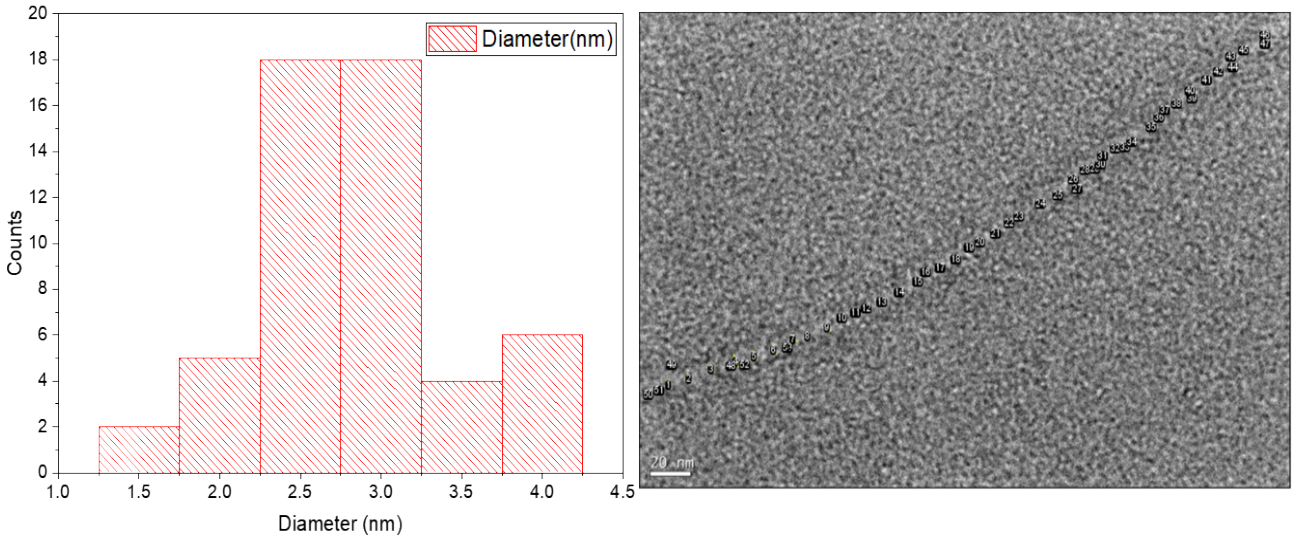

Figure S34. 200 kV JEM-2100HR TEM, histogram for diameter estimation of PNTs along with corresponding micrograph.

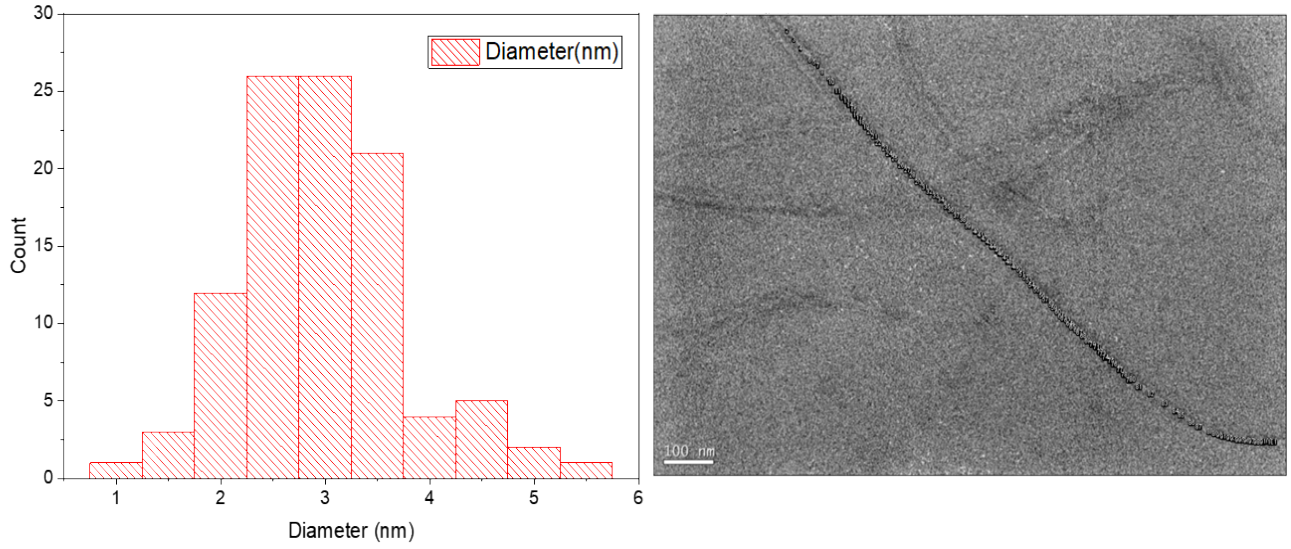

Figure S35. 200 kV JEM-2100HR TEM, histogram for diameter estimation of PNTs.

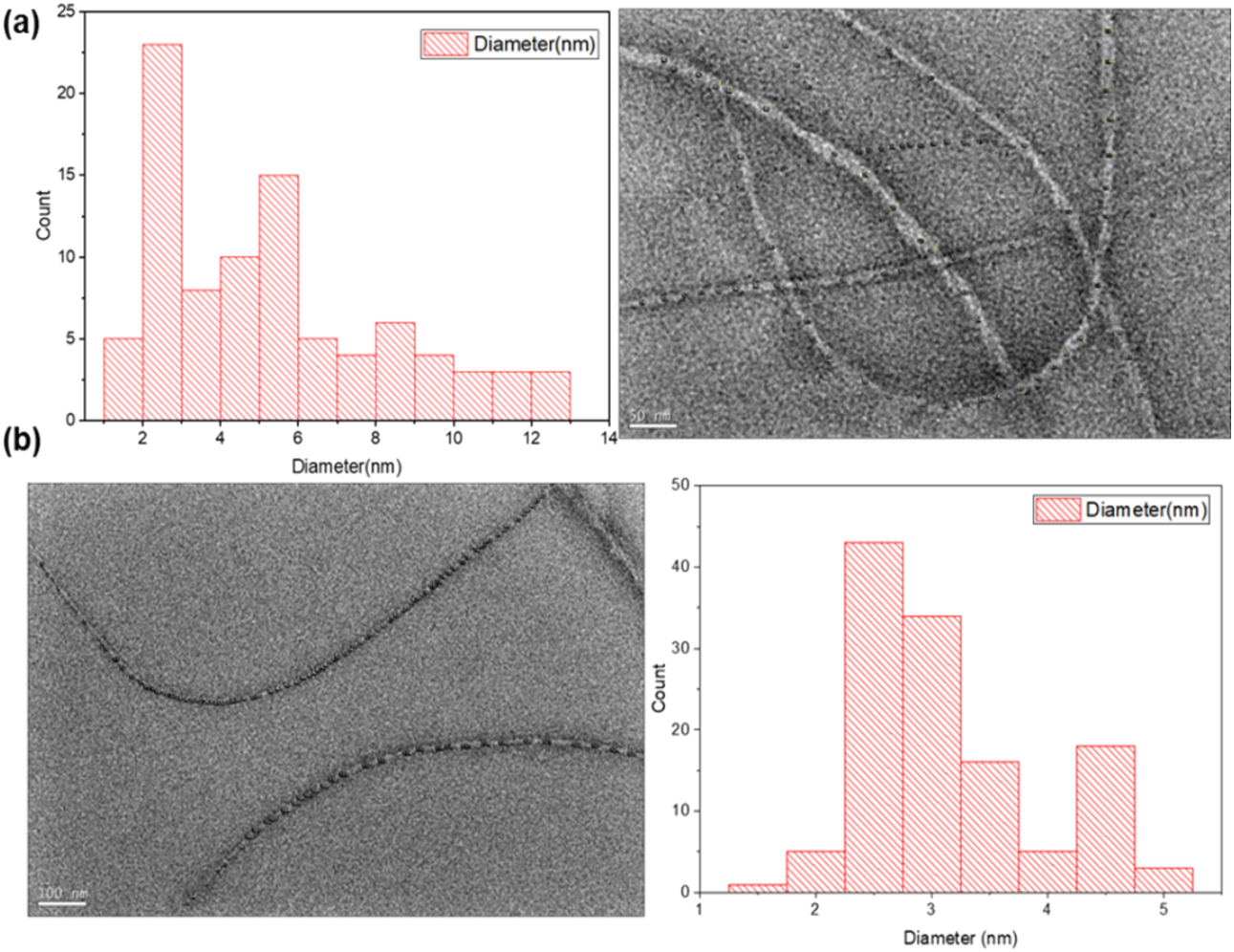

Figure S36. (a-b) 200 kV JEM-2100HR TEM, histogram for diameter estimation of PNTs.

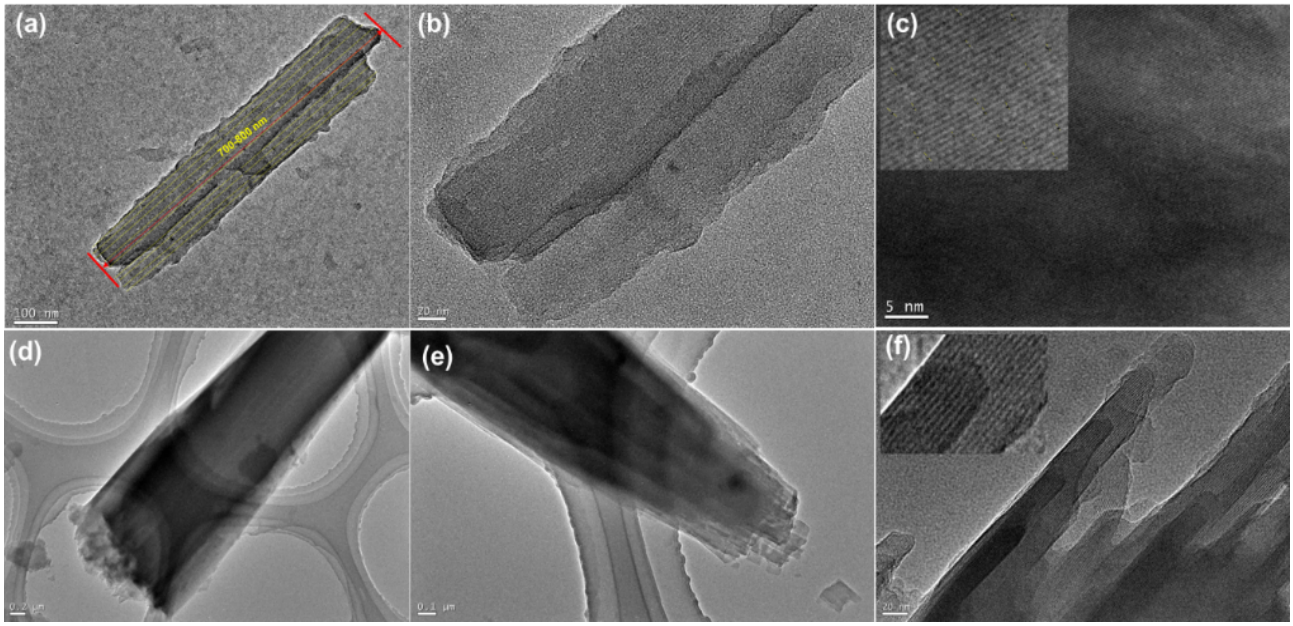

Figure S37. 200 kV JEM-2100HR TEM, **(a-c)** micrographs of PNTs suspension in ethyl acetate and **(d-f)** are in EtOH.

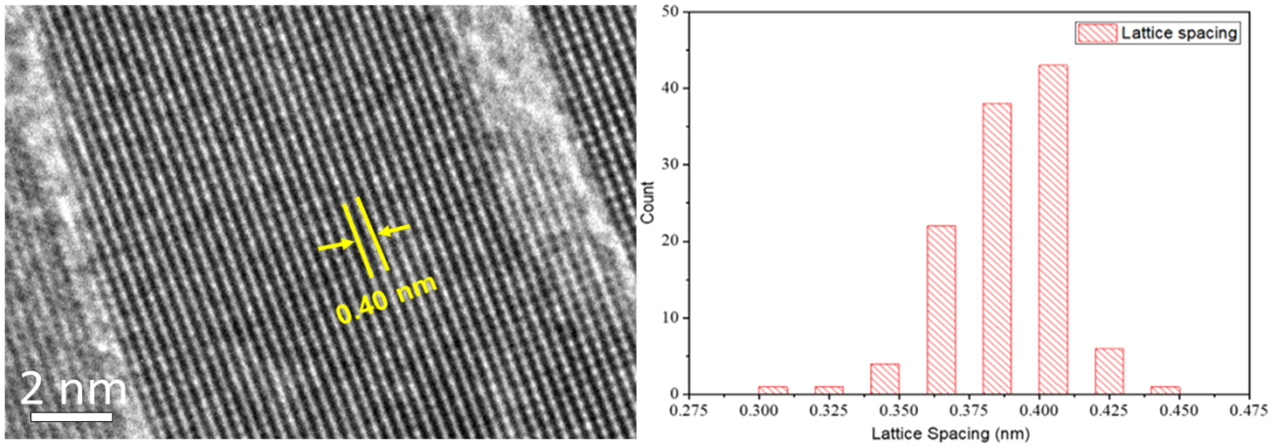

Figure S38. HR-TEM micrograph and histogram for estimation of lattice spacing.

6. SAED Data

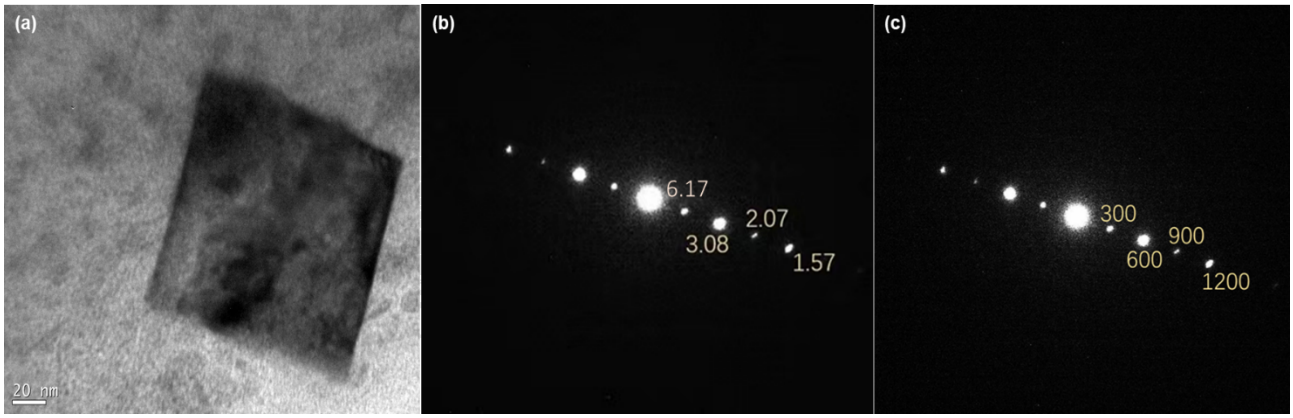

Figure S39. (a) TEM-BF image of single crystal of PNTS **(b)** SAED pattern of the same crystal with d-spacing and **(c)** is the SAED pattern with miller indexes.

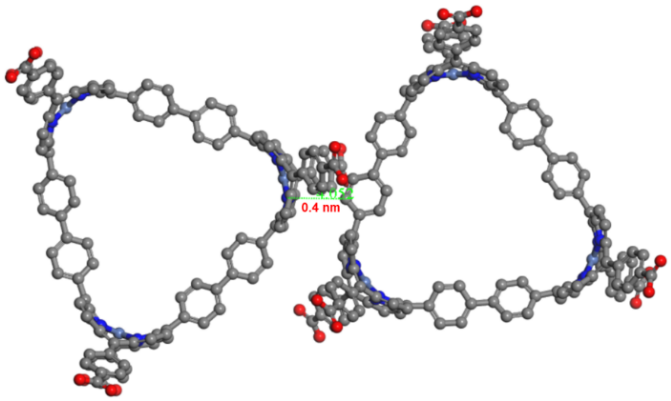

Figure S40. The model of PNTs showing lattice spacing 4.052 Å, which is consistent with interplanar distancing i.e, 0.4 nm of resolved lattice fringes in HRTEM.

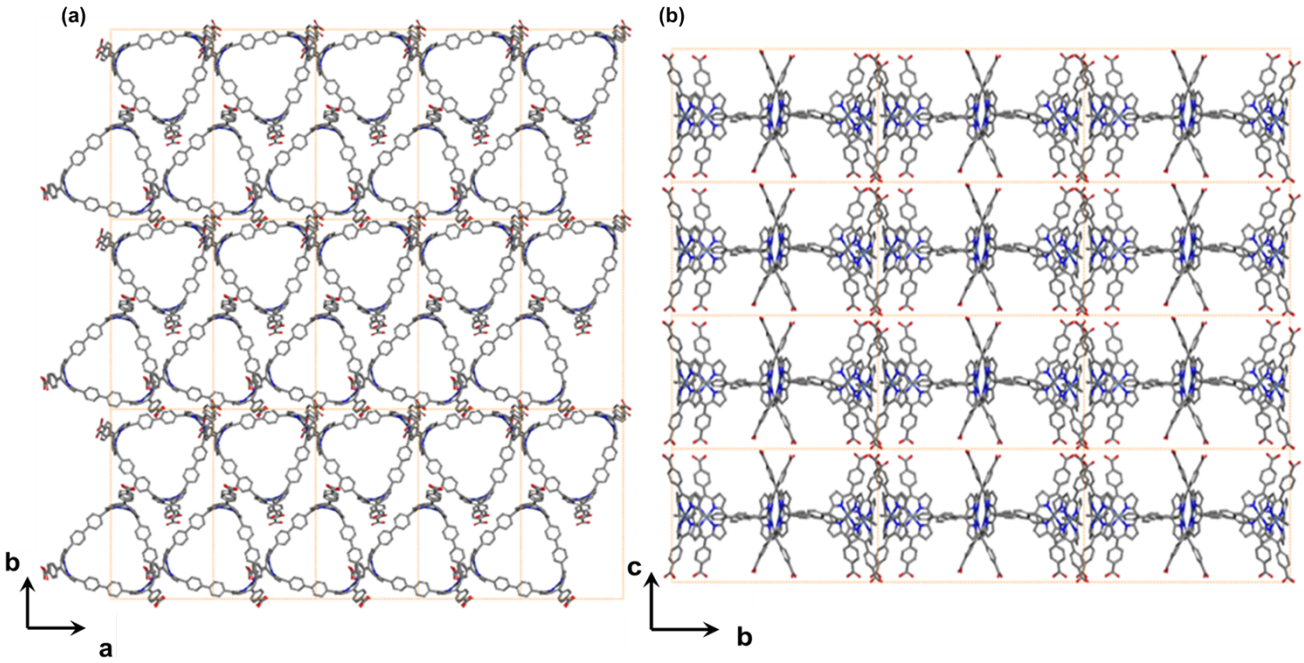

Figure S41. The crystal model of PNTs based on SAED results **(a)** Top view, **(b)** side view.

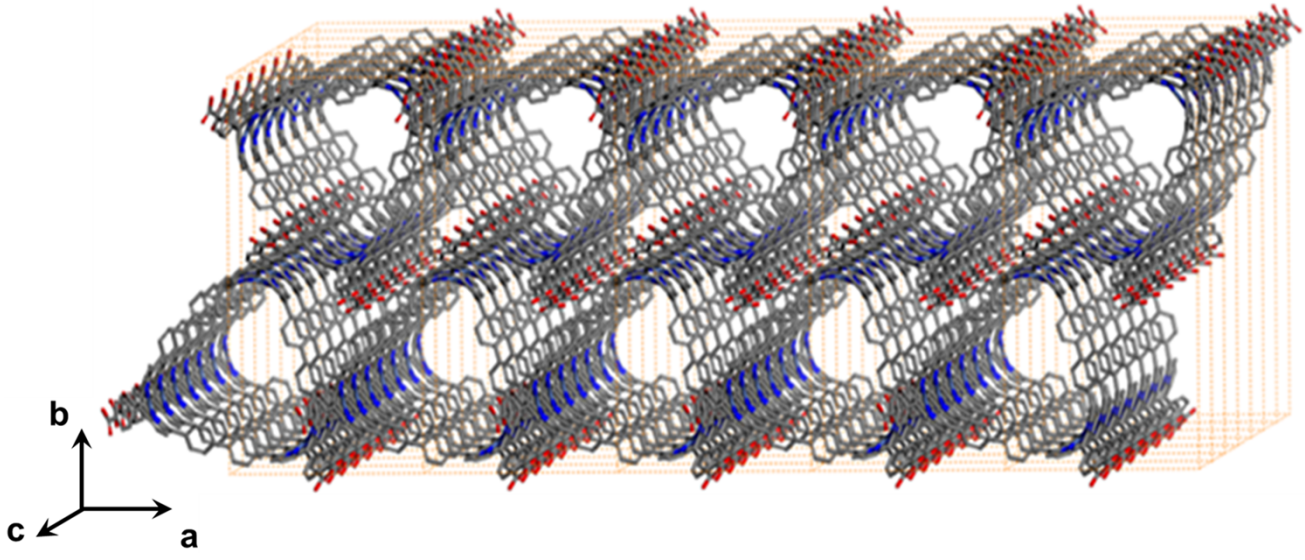

Figure S42. The 3D view of PNTs crystals crystal model of PNTs based on SAED results.

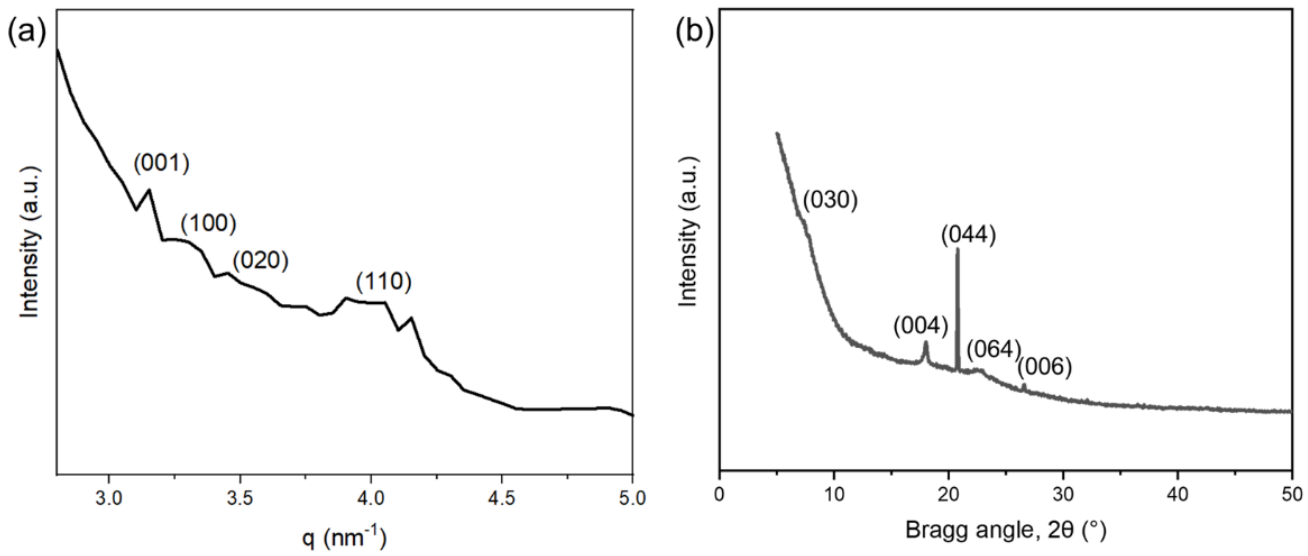

Figure S43. 1D **(a)** SAXD and **(b)** WAXD profiles of PNTs crystals.

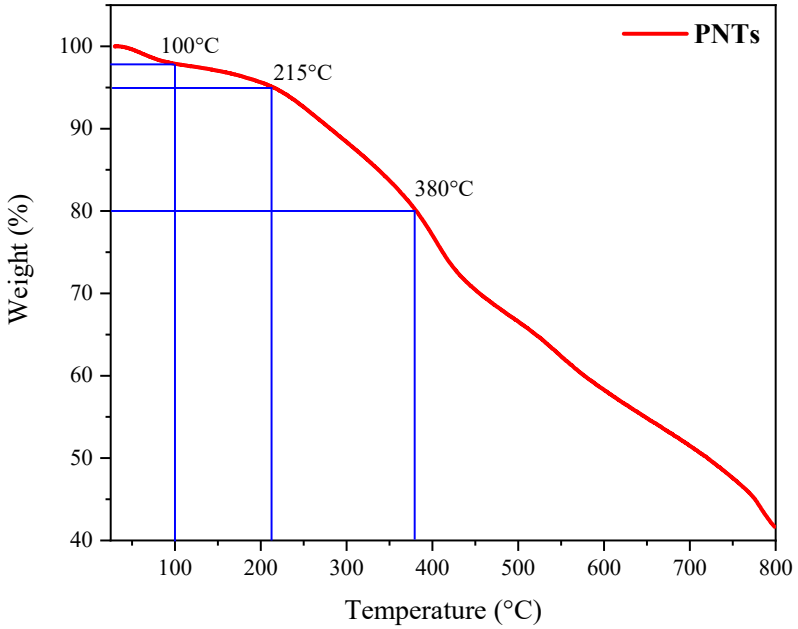

Figure S44. TGA of self-assembled Porphyrin nanotubes.

In the TGA graph the % weight loss at several temperatures have been described in **Figure S44**. We assume that the first 2 % weight loss before 100°C is due to the loss of water molecules present on the outer surface of PNTs (approximately $3H_2O$ per trimer). Then onward heating up to 215°C resulted in another ~3% weight loss due to evaporation of the entrapped solvents like 1,4-dioxane, ethanol and water molecules (probably 1dioxane per trimer, or 1EtOH per trimer and $2H_2O$ per trimer). Then from 215-380°C, the pronounced weight loss (~15%) could be associated to the destruction of hydrogen bonds accompanied with the deprotonation of carboxylic (COOH) group during the heating process. Moreover, at this stage weight loss is not very sharp, which suggested that there were still some solvent molecules coming out of PNTs. Owing to the simultaneous decomposition of **3** along with the loss of solvents, the exact percentage of solvent molecules at this stage could not be estimated precisely. While the next stage (from 380 to 800°C) includes the decomposition of porphyrin scaffold.

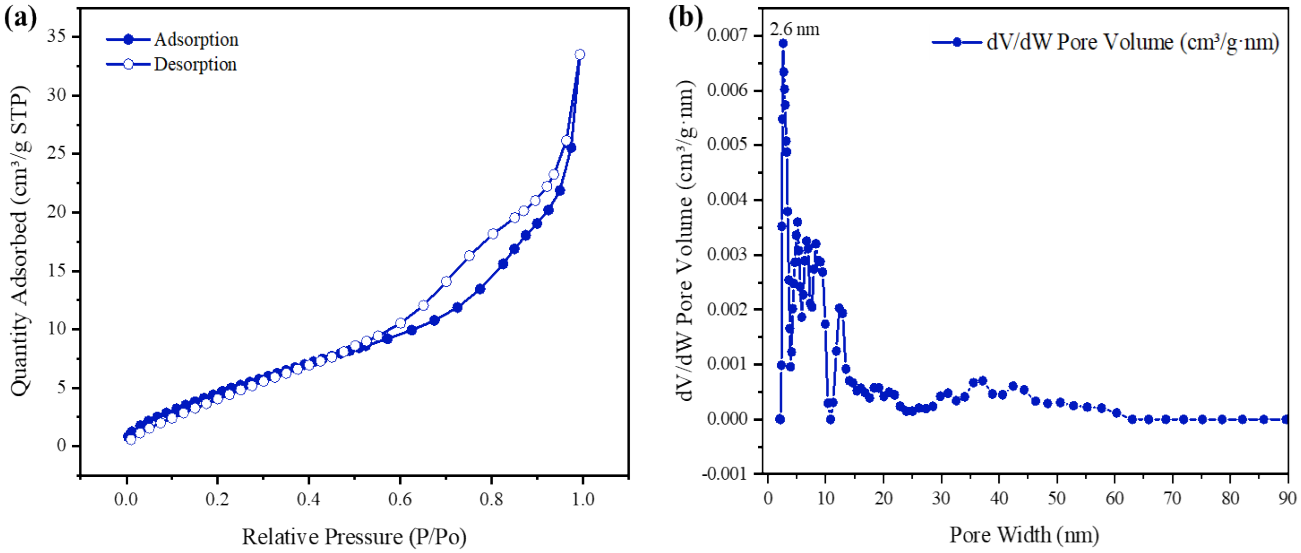

Figure S45. (a) N_2 adsorption/desorption isotherm curve (77 K) of PNTs and **(b)** the curve of pore size distribution.

References

1 K. Ogawa, J. Dy and Y. Kobuke, *J. Porphyr. Phthalocyanines*, 2005, **9**, 735–744.

2 B. J. Littler, M. A. Miller, C.-H. Hung, R. W. Wagner, D. F. O'Shea, P. D. Boyle and J. S. Lindsey, *J. Org. Chem.*, 1999, **64**, 1391–1396.

3 T. S. Balaban, R. Goddard, M. Linke-Schaetzel and J.-M. Lehn, *J. Am. Chem. Soc.*, 2003, **125**, 4233–4239.

4 J. M. Quimby and L. T. Scott, *Adv. Synth. Catal.*, 2009, **351**, 1009–1013.

5 B. K. Tripuramallu, S. Goswami and I. Goldberg, *Cryst. Growth Des.*, 2018, **18**, 230–241.